VTRC
Virginia Transportation Research Council

We Bring Innovation to Transportation

Welding of ASTM A709 50CR Using Austenitic Filler Wires With Varying Heat Inputs and Maximum Interpass Temperatures

http://www.virginiadot.org/vtrc/main/online_reports/pdf/20-r24.pdf

JAMES M. FITZ-GERALD, Ph.D.
Professor

SEAN R. AGNEW, Ph.D.
Professor

XUEMENG XIA
Graduate Student

Department of Materials Science and Engineering
University of Virginia

Final Report VTRC 20-R24

VIRGINIA TRANSPORTATION RESEARCH COUNCIL
530 Edgemont Road, Charlottesville, VA 22903-2454
vtrc.virginiadot.org

Standard Title Page—Report on State Project

Report No.: VTRC 20-R24	Report Date: March 2020	No. Pages: 54	Type Report: Final Contract	Project No.: 109736
			Period Covered:	Contract No.:

Title:
Welding of ASTM A709 50CR Using Austenitic Filler Wires With Varying Heat Inputs and Maximum Interpass Temperatures

Key Words: ASTM A1010, A709, bridge, girder, grade 50CR, heat input, interpass temperature, stainless steel, welding

Author(s):
James M. Fitz-Gerald, Ph.D., Sean R. Agnew, Ph.D., and Xuemeng Xia

Performing Organization Name and Address:
Virginia Transportation Research Council
530 Edgemont Road
Charlottesville, VA 22903

Sponsoring Agencies' Name and Address:
Virginia Department of Transportation
1401 E. Broad Street
Richmond, VA 23219

Supplementary Notes:

Abstract:

ASTM A709 Grade 50CR, also known as ASTM A1010, is a structural steel developed to address the corrosion issues associated with the use of traditional weathering steels, especially in environments involving combined prolonged wetness and chlorine salts. The fabrication of bridge girders from Grade 50CR has largely relied on the use of 309L solid filler wire with heat inputs up to 55 kJ/in and maximum interpass temperatures up to 450 °F for 1 in thick plate. The purpose of this project was to determine if higher heat inputs could be used when welding 50CR and to evaluate several filler wire materials that could be used during plate girder fabrication. Three groups of 50CR plates were used in this study: sixteen 1/2-inch thick welded 50CR plates, twelve 1 in thick welded 50CR plates, and two welded AWS D1.5 prequalification record (PQR) plates. The testing performed in this study revealed the following:

- The ductile to brittle transition temperature (DBTT) of the 50CR base plate was measured to be -40 °F.
- A range of austenitic stainless steel filler wires can be used to successfully weld 50CR. In this study, 309LC (metal cored wire), 309LSi (Si added for flowability and appearance), and 316L (Mo added for enhanced corrosion resistance) were found to be viable alternatives to the incumbent filler wire, 309L.
- Use of 309L filler wires for 1/2 in plates results in submerged arc welds (SAW) which are borderline with respect to impact energy at the high heat input level of 75 kJ/in, over the temperature range investigated. Lower heat inputs (e.g., 55 kJ/in previously shown effective) are recommended. Similar results were obtained for welds in 1/2 in plates produced with 309LSi and 316L.
- Heat inputs of up to 75 kJ/in at all interpass temperatures explored (up to 450 °F) can be used to weld 1/2-inch plates with 309LC filler wire. The enhanced toughness and low DBTT of welds in 1/2 in plates formed using 309LC filler wire appears to be due to the mitigation of large, aligned δ-ferrite grain formation during solidification. Such large, aligned grains otherwise serve as preferred crack paths in welds.
- Heat inputs of 90 kJ/in and interpass temperatures of up to 450 °F can be used for all four of the filler wires investigated (309L, 309LC, 309LSi, and 316L) for 1 in thick plate.

It is recommended that when 50CR is considered for bridges in specific corrosive environments due to its corrosion resistance, improved mechanical properties, and lifetime cost, the aforementioned findings be incorporated in the guidance documents. The availability of alternatives to the conventional solid 309L filler wire currently used to weld 50CR allows more vendors, eliminating the requirement for sole source justification and opening broader possibilities to satisfy Buy America requirements for federally funded bridge projects. Finally, 309LC (metal-cored filler wire) outperformed the solid filler wires examined in this study with respect to production (higher deposition rates and fewer required passes) and mechanical properties (especially impact toughness) of the resulting welds.

FINAL REPORT

WELDING OF ASTM A709 50CR USING AUSTENITIC FILLER WIRES WITH VARYING HEAT INPUTS AND MAXIMUM INTERPASS TEMPERATURES

James M. Fitz-Gerald, Ph.D.
Professor

Sean R. Agnew, Ph.D.
Professor

Xuemeng Xia
Graduate Student

Department of Materials Science and Engineering
University of Virginia

VTRC Project Manager
Stephen R. Sharp, Ph.D., P.E., Virginia Transportation Research Council

Virginia Transportation Research Council
(A partnership of the Virginia Department of Transportation
and the University of Virginia since 1948)

Charlottesville, Virginia

March 2020
VTRC 20-R24

DISCLAIMER

The project that is the subject of this report was done under contract for the Virginia Department of Transportation, Virginia Transportation Research Council. The contents of this report reflect the views of the authors, who are responsible for the facts and the accuracy of the data presented herein. The contents do not necessarily reflect the official views or policies of the Virginia Department of Transportation, the Commonwealth Transportation Board, or the Federal Highway Administration. This report does not constitute a standard, specification, or regulation. Any inclusion of manufacturer names, trade names, or trademarks is for identification purposes only and is not to be considered an endorsement.

Each contract report is peer reviewed and accepted for publication by staff of the Virginia Transportation Research Council with expertise in related technical areas. Final editing and proofreading of the report are performed by the contractor.

ABSTRACT

ASTM A709 Grade 50CR, also known as ASTM A1010, is a structural steel developed to address the corrosion issues associated with the use of traditional weathering steels, especially in environments involving combined prolonged wetness and chlorine salts. The fabrication of bridge girders from Grade 50CR has largely relied on the use of 309L solid filler wire with heat inputs up to 55 kJ/in and maximum interpass temperatures up to 450 °F for 1 in thick plate. The purpose of this project was to determine if higher heat inputs could be used when welding 50CR and to evaluate several filler wire materials that could be used during plate girder fabrication. Three groups of 50CR plates were used in this study: sixteen 1/2-inch thick welded 50CR plates, twelve 1 in thick welded 50CR plates, and two welded AWS D1.5 prequalification record (PQR) plates. The testing performed in this study revealed the following:

- The ductile to brittle transition temperature (DBTT) of the 50CR base plate was measured to be -40 °F.

- A range of austenitic stainless steel filler wires can be used to successfully weld 50CR. In this study, 309LC (metal cored wire), 309LSi (Si added for flowability and appearance), and 316L (Mo added for enhanced corrosion resistance) were found to be viable alternatives to the incumbent filler wire, 309L.

- Use of 309L filler wires for 1/2 in plates results in submerged arc welds (SAW) which are borderline with respect to impact energy at the high heat input level of 75 kJ/in, over the temperature range investigated. Lower heat inputs (e.g., 55 kJ/in previously shown effective) are recommended. Similar results were obtained for welds in 1/2 in plates produced with 309LSi and 316L.

- Heat inputs of up to 75 kJ/in at all interpass temperatures explored (up to 450 °F) can be used to weld 1/2-inch plates with 309LC filler wire. The enhanced toughness and low DBTT of welds in 1/2 in plates formed using 309LC filler wire appears to be due to the mitigation of large, aligned δ-ferrite grain formation during solidification. Such large, aligned grains otherwise serve as preferred crack paths in welds.

- Heat inputs of 90 kJ/in and interpass temperatures of up to 450 °F can be used for all four of the filler wires investigated (309L, 309LC, 309LSi, and 316L) for 1 in thick plate.

It is recommended that when 50CR is considered for bridges in specific corrosive environments due to its corrosion resistance, improved mechanical properties, and lifetime cost, the aforementioned findings be incorporated in the guidance documents. The availability of alternatives to the conventional solid 309L filler wire currently used to weld 50CR allows more vendors, eliminating the requirement for sole source justification and opening broader possibilities to satisfy Buy America requirements for federally funded bridge projects. Finally, 309LC (metal-cored filler wire) outperformed the solid filler wires examined in this study with respect to production (higher deposition rates and fewer required passes) and mechanical properties (especially impact toughness) of the resulting welds.

FINAL REPORT

WELDING OF ASTM A709 50CR USING AUSTENITIC FILLER WIRES WITH VARYING HEAT INPUTS AND MAXIMUM INTERPASS TEMPERATURES

James M. Fitz-Gerald, Ph.D.
Professor

Sean R. Agnew, Ph.D.
Professor

Xuemeng Xia
Graduate Student

Department of Materials Science and Engineering
University of Virginia

INTRODUCTION

Due to the poor corrosion resistance of mild steel, various steels with comparable mechanical properties have been explored as replacements in structural applications.[1] Although weathering steels can meet the mechanical property requirements of bridge girders, they fail to meet the corrosion resistance necessary in environments with prolonged moisture or chloride containing salts and would thus need to be periodically coated with a protective barrier every twenty years.[1,2] A more corrosion resistant alternative was sought. Traditional austenitic (and even duplex austenitic-ferritic) stainless steels are more expensive, while traditional ferritic stainless steels can exhibit poor weldability due to the excessive grain growth in the heat affected zone (HAZ).[3-13] Dual phase (ferritic-martensitic) stainless steels, such as ASTM A709 Grade 50CR (50CR), formerly ASTM A1010, have been offered as a possible solution. Designed to form a protective scale that greatly reduces the atmospheric corrosion rate, 50CR was determined by various studies to be more cost-effective over the lifetime of a bridge in comparison with weathering steel.[1,14-16] A predecessor alloy, which was designated 3CR12, had a prescribed amount of titanium (Ti) added to the alloy composition to render the material "stabilized" relative to sensitization to grain boundary corrosion and cracking phenomena. The idea was that Ti would bind excess carbon (C) in the alloy and thereby avoid unwanted chromium carbide formation on grain boundaries. Detailed study showed that this well-intentioned alloy design strategy was not effective, and therefore, the requirement for Ti-stabilization is not included in the specification of 50CR.[17-20]

In 2004, the first 50CR multi-cell box girder bridge was erected in Williams, California as part of the Innovative Bridge Research and Construction Program.[21] Following its construction, several other state Department of Transportations (DOTs) as well as a commercial entity began using 50CR in bridge girder applications.[22] Early work on 3CR12 showed that the use of austenitic stainless steel filler wire materials was preferred over homogeneous welding,

due to problems with cracking of the latter type of weld.[8] Work performed by the Oregon DOT established the use of a specific austenitic stainless steel alloy, ER309L, filler wire as the standard procedure for the fabrication of 50CR bridge girders. The Oregon study focused on improving fabrication costs by using a heat input of 55 kJ/in and increasing the maximum interpass temperature from the range of 210 to 225 °F to maximum interpass temperatures of 225 (control), 300, 400, and 450 °F on 1 in thick plate. The welds performed with any combination of these welding parameters were observed to pass the mechanical property requirements set by AWS D1.5.[23] Given that the interpass temperatures used in the Oregon study exceed the manufacturer's recommendations for maximum interpass temperature (210 – 225 °F), at 70 kJ/in for 1 in thick plate, the actual limits remain undetermined.[24] Increasing the limits on the maximum interpass temperature and the heat input can lead to a greater fabrication efficiency and lower overall cost, but could cause detrimental effects to the mechanical properties, such as a loss in strength and/or impact energy due to effects on the microstructure.

Because the use of 50CR is intended for the construction of maintenance-free girders, microstructural analysis of the welds is important to explain the observed performance of the welded structures and, perhaps more importantly, to determine if any issues may arise after the erection of the bridge.[22] Welding produces distinct microstructural regions: the fusion zone, the HAZ, and the base material.[25] The fusion zone is a mixture of the base material and the filler wire and is characterized by the level of dilution experienced by the filler metal. Many factors can affect the dilution, including the type of filler wire, heat input, maximum interpass temperature, number of passes, and type of welding technique.[26,27] The dilution consequently affects the phase content of the fusion zone, due to the changing balance of phase stabilizers, especially chromium (Cr) and nickel (Ni).[28-33] The phases that will be present after welding are often predicted using the Schaeffler[31], DeLeong[33], or WRC-1992[33] constitution diagrams. The latter two are applicable to higher Cr_{eq} and Ni_{eq} ranges than those in this study, so the present report will only reference the Schaeffler diagram.

It is well established that welds which only contain the austenite phase (i.e., less than ~5 vol.% residual δ-ferrite) are prone to hot-cracking, presumably due to the higher solubility of the δ-ferrite phase for tramp elements, like sulfur, which are associated with such solidification cracking phenomena.[34,35] δ-ferrite is a solid solution of C in BCC Fe that has the same structure as α-ferrite but it is stable only at temperatures above ~ 2500 °F and melts at ~ 2800 °F. On the other hand, it is a matter of controversy as to whether higher levels of residual δ-ferrite result in lower mechanical properties of austenitic welds themselves.[31,34,36,37] Indeed, strong reductions in weld toughness and increases in the ductile to brittle transition temperature (DBTT) have been observed for austenitic welds of a martensitic stainless steel.[36] However, it has also been shown that only very high (> 50%) residual δ-ferrite contents are correlated with strong reductions in the toughness of a lean, duplex stainless steel.[37] This wide range of observations suggests other factors, such as fusion zone microstructure morphology may have an even more important and controlling influence than simply residual δ-ferrite content.

Austenitic filler metals can solidify according to four different cases.[38] The *A* case involves completely austenitic solidification. The *AF* cases begin as austenite and then some of the high temperature, δ-ferrite phase forms in the interdendritic regions during the final stages of solidification. Conversely, *FA* cases begin the solidification process as δ-ferrite, and the last

liquid to solidify does so as austenite. Finally, the *F* cases complete the solidification process as δ-ferrite. The δ-ferrite is thermodynamically unstable at temperatures below 2500°F and will tend to undergo a solid-state phase transformation to austenite during cooling to room temperature. All of these pathways can result in welds that are primarily austenite; however, the microstructures resulting from the various welding conditions can be quite distinct. A new technique known as electron-backscattered diffraction (EBSD) within a scanning electron microscope has enabled both the phase (crystal structure) and crystal orientation of the phases to be determined.[39] Using EBSD, it has been shown that despite microstructures with radically distinct morphologies, the austenite and retained ferrite regions present in both *F* and *FA* type welds are crystallographically related to each other through the Nishiyama-Wasserman (NW) or Kurjdumov-Sachs (KS) orientation relationships.[39] In *FA* types, the weld metal has a dendritic appearance with δ-ferrite residing in the interdendritic regions. All of the welds examined in the present study will be shown to follow the *F* case, which leads to large (here denoted prior δ-ferrite) grains, which largely transform into austenite having a basket-weave (Widmanstätten) type microstructure during cooling.

The results of this study on 50CR have led to the hypothesis that it is not the absolute phase fraction of retained δ-ferrite that is most critical. Rather, it is the scale and morphology of the microstructure that must be controlled in order to avoid embrittlement of the weld fusion zone.

PURPOSE AND SCOPE

The purpose of this project was to 1) determine if a higher heat input combined with the maximum interpass temperature up to 450 °F could be used when welding 50CR, and 2) evaluate several filler wire materials that could be used during plate girder fabrication. Although the producer of 50CR recommends the use of ER308L, ER309L, ER316L, and their higher silicon content counterparts,[24] ER309L has by far been the most widely used filler wire for welding 50CR plate girders.[40] To address these two areas, discussion with industry experts, a literature review, compositional testing, metallurgical analysis and mechanical testing were all performed. When applicable, testing was performed in compliance with the appropriate standard. All of the 50CR test plates were welded at a traditional bridge fabrication shop. After fabricating test plates, all the testing was performed in a controlled laboratory setting.

METHODS

Ten-filler wire manufacturers and distributers were contacted to find filler wires appropriate for submerged arc welding (SAW) of 50CR. Factors that were considered included: alloy recommendations by the plate producer, country of origin, cost, availability, and lead time. Four different 3/32 in filler wires were ultimately selected: ER309L (309L), ER309LSi (309LSi), and ER316L (316L) solid welding wire provided by Lincoln Electric, and ER309L metal cored welding wire (309LC) by Select Arc. The three distinct compositions are listed in Table 1 (309LC has the same nominal composition as 309L). Characterization of the four-filler wire types involved using the Scanning Electron Microscope (SEM) to observe the microstructure and Electron Dispersive Spectroscopy (EDS) mapping within the SEM to determine the distribution of elements present. These methods are detailed below.

Table 1. Nominal compositions of the filler wires used in this study per AWS A5.9 requirements in weight % (wt %)

Filler Wire	Chromium	Nickel	Molybdenum	Manganese	Silicon
ER309L	23.0 – 25.0	12.0 – 14.0	0.75	1.0 – 2.5	0.30 – 0.65
ER309LSi	23.0 – 25.0	12.0 – 14.0	0.75	1.0 – 2.5	0.65 – 1.00
ER316L	18.0 – 20.0	11.0 – 14.0	2.0 – 3.0	1.0 – 2.5	0.30 – 0.65

Note: Filler wire 309L and 309LC have the same nominal composition

Welded Plate Fabrication

Plate fabrication was performed by a commercial bridge girder fabricator in accordance with AASHTO/AWS D1.5. All welding was performed with SAW with no pre-heat used at the start of any of the welding. Single and double V groove welds were used for 1/2 in thick plates (referred to as Group 1) and 1 in thick plates (referred to as Group 2), and for 1 in thick PQR plates (referred to as Group 3), respectively.[41] The aforementioned 3/32 in filler wires were utilized to weld the 50CR base plates together: 309L, 309LSi, and 316L solid welding wire, and 309LC metal-cored welding wire. Lincolnweld 880M® flux was used in all cases.

Based on published literature, communications with VDOT, Virginia Transportation Research Council (VTRC), Turner-Fairbank Highway Research Center (TFHRC), a 50CR steel plate producer, and an experienced 50CR bridge girder fabricator, heat inputs of 50 and 75 kJ/in, and maximum interpass temperatures of 125, 300, and 450 °F were selected for welding Group 1 plates.[23,24] The maximum interpass temperature is the temperature that the plate must achieve before a subsequent weld pass can be laid and is measured at the weld centerline. The lowest interpass temperature was chosen based on prior welding experience from VDOT's Route 340 Bridge constructed with 50CR steel plate girders. In order to achieve an interpass temperature of 450 °F the fabricator heated the steel plate with an oxyacetylene torch. Heat inputs of 70 kJ/in and 90 kJ/in and maximum interpass temperature of 300 and 450 °F were used on the Group 2 plates. Based on the results of Charpy V-notch (CVN) testing of Group 1 welds (detailed below), a third group of two 1 in thick plates, (Group 3) was tested in accordance with the AWS D1.5 Welding Procedure: Specification Plate A fabrication requirements using 309L and 309LC with a maximum heat input of 90 kJ/in and a maximum interpass temperature of 450 °F.[41] A list of all the combinations of parameters employed in this study can be found in Table 2.

Table 2. List of welding parameter combinations used in the study

Group	Plate Thickness (in)	Filler Wires Used	Heat Input (kJ/in)	Maximum Interpass Temp. (°F)
1	1/2	309L, 309LC, 309LSi, 316L	50	300
1	1/2	309L, 309LC, 309LSi, 316L	75	125
1	1/2	309L, 309LC, 309LSi, 316L	75	300
1	1/2	309L, 309LC, 309LSi, 316L	75	450
2	1	309L, 309LC, 309LSi, 316L	70	300
2	1	309L, 309LC, 309LSi, 316L	90	300
2	1	309L, 309LC, 309LSi, 316L	90	450
3 (PQR)	1	309L, 309LC	90	450

Sample Machining

Samples for metallurgical analysis and mechanical testing were machined from the plates in the orientations listed below in Figure 1. The sample configuration maps for the plates from Groups 1, 2 and 3 are shown in Appendix A: Cut Diagrams.

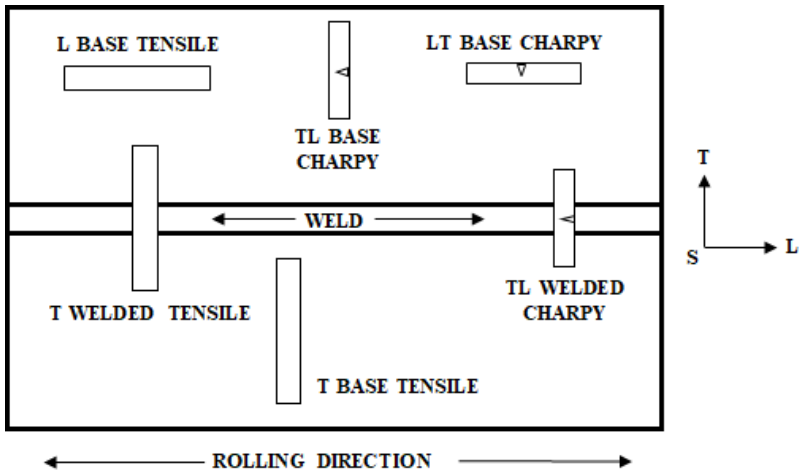

Figure 1. Schematic illustration of sample orientations with reference to a coordinate system defined by the L (longitudinal/rolling), and T (long transverse), and S (short-transverse) directions (the schematic is an indication of the types of samples used in Group 1 and 2, not the actual cut plan)

Compositional Analysis

Compositional analysis was performed on a 1 in x 1/2 in x 1/2 in sample of the 50CR base plate from Group 1 in accordance with ASTM E1019[42] and ASTM E1479[43]. Filler wire samples of 309L and 309LC were analyzed in accordance with ASTM E1019 and ASTM E1479, while samples of 309LSi and 316L were analyzed using Energy Dispersive Spectroscopy (EDS).

The composition of the 309L, 309LSi, and 316L solid filler wires was estimated by semi-quantitative EDS scans in the SEM. In addition, the EDS scans were used to estimate the composition of fifteen regions (400 by 500 microns) on the face perpendicular to the longitudinal direction starting from the edge of the weld and moving towards the center of each Group 1 plate using scribed line and micro-hardness indention points, spaced 0.025 in apart, as markers. The location of the indention points was 0.125 in from the edge of the sample, as shown in Figure 2. EDS in the SEM operates by measuring the relative number of X-ray photons characteristic of each element, which are emitted by the material when irradiated by electrons.[44]

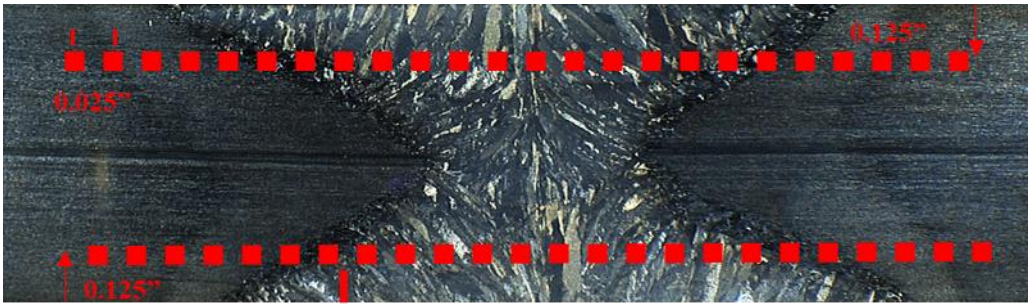

Figure 2. Welded 1/2 in plate with the reference scribe (shown by the line) and location of micro-Vickers hardness indention points shown

The compositions obtained with EDS were used to estimate the level of dilution (D) of Cr and Ni using Equation 1, where C_{fz}, C_{bm}, C_{fm} are the concentrations of an element in the fusion zone, base metal, and filler metal respectively.[26] The concentrations of these two elements were used because they had the largest concentration difference between the base metal and the filler wire, thus decreasing the uncertainty in the dilution estimates.

$$D = (C_{fz} - C_{fm}) / (C_{bm} - C_{fm}) \quad \text{(Equation 1)}$$

The compositions determined by the EDS area scans of the Group 1 plates were used together with the Schaeffler diagram to predict the microstructure of the fusion zone.[31]

Microstructural Analysis

Conventional Metallography

Samples that spanned across the HAZ were obtained from the planes parallel to the longitudinal (L), long-transverse (T), and short-transverse (S) directions, as shown in Figure 1, from each group of 50CR plates received. These samples were then ground and polished to a 0.05 micron finish and etched using Vilella's reagent, prepared in accordance to ASTM E407.[45] Conventional optical microscopy (OM) and image processing was used to determine the ferrite volume fraction. OM micrographs were converted to a binary black and white 2D image and the pixels of the ferrite were counted and converted to an area percentage. This area ferrite content was assumed equivalent to the volume percentage of residual δ-ferrite in the welds.

Four inches were cut and discarded from either side of the Group 1 and 2 plates to ensure that the steady-state condition for submerged arc welding had been reached, as shown in Appendix A. All of the weld cross-section samples were polished to a 0.05 micron finish. The welded samples were etched using Kalling's No. 2 reagent, prepared in accordance with ASTM E407.[45] OM was used to take micrographs of the various microstructural regions. Image processing was used to determine the amount of ferrite present in fifteen areas of 250 by 300 microns. Scribed lines and micro-hardness indention points, shown in Figure 2, were used to ensure that the same region was analyzed with EDS. Three macro-etch samples were prepared in accordance with AASHTO/AWS D1.5 Section 5.18.2 and analyzed according to Section 5.19.3, for each plate in Group 3.[41]

X-ray Diffraction

One longitudinal face sample was taken from the each of the 1/2 in and 1 in thick 50CR base plates as well as one transverse face sample from each of the welded Group 3 plates, ground and polished to a 1200 grit finish, and analyzed using conventional X- Ray Diffraction (XRD) to estimate the volume fractions of the phases present.

Mechanical Testing

Hardness Testing

Micro-hardness testing was performed using a Vickers testing machine using a load time of 15 seconds and a load of 500 g. Data points were taken 0.025 in apart. One line of micro-hardness data was taken through the thickness on two 50CR base material samples from the Group 1 plates, Group 2 plates, and the Group 3 plates, for a total of six samples. Two lines of data were taken across the weld (0.125 in from the top and bottom surfaces) the S direction of each of the Group 1 welded plates, as seen in Figure 2. One line of data was taken across the weld 0.25 in in the S direction of each of the Group 2 welded plates.

Tensile Testing

Tensile testing was performed on the 1/2 in thick 50CR in the L and T orientations, as indicated in Figure 1. The strain rates imposed on the samples involve a ramping up program in accordance with ASTM A370, which respects the relative strain rate insensitivity of steels during low temperature deformation.[46] Samples with a 2 in gage length were machined in accordance with the ASTM A370 sheet-type sample geometry, shown in Figure 3a. Five samples were tested for each condition. The same sort of tensile testing was performed on each of the Group 1 plates in the T orientation with the weld placed in the middle of the gage length. 1/2 in samples were tested in sets of five on a load frame with a capacity of 55-kips. In the same way, three samples, shown in Figure 3b, from Group 2 plates were tensile tested in the T orientation using a load frame with a capacity of 110-kips. Finally, one all-weld-metal tensile and two reduced-section tensile samples were machined and tested from each Group 3 plate in accordance with AASHTO/AWS D1.5 Section 5.18.1 and Section 5.18.4.[41] The samples were then analyzed in accordance with Section 5.19.1 and 5.19.4, which leads to the reporting tensile strength, reduction in area, and percent elongation for both types of tensile samples and yield strength for just the all-weld-metal tensile sample.

Charpy V-notch (CVN) Testing

Charpy V-notch (CVN) testing of impact toughness (energy absorption) was performed on 1/2 in thick 50CR base metal in the LT and TL orientations, indicated in Figure 1. The length of the LT sample is oriented in the longitudinal (L) direction and the V notch (cracking direction) is parallel to the transverse (T) direction. The TL sample is oriented in the opposite manner. Twenty full-size CVN samples of each orientation were machined from one of the Group 1 welded plates far enough away from both the edge of the plate and the weld to be representative of the base metal performance, in accordance to ASTM E23.[47] Three samples were tested at 40

°F, the temperature indicated by ASTM A709 for Zone 2.[48] Samples were tested at each of the following additional temperatures: -100, -80, -60, -30, -10, and 10 °F, to determine the ductile to brittle transition temperature (DBTT) behavior.

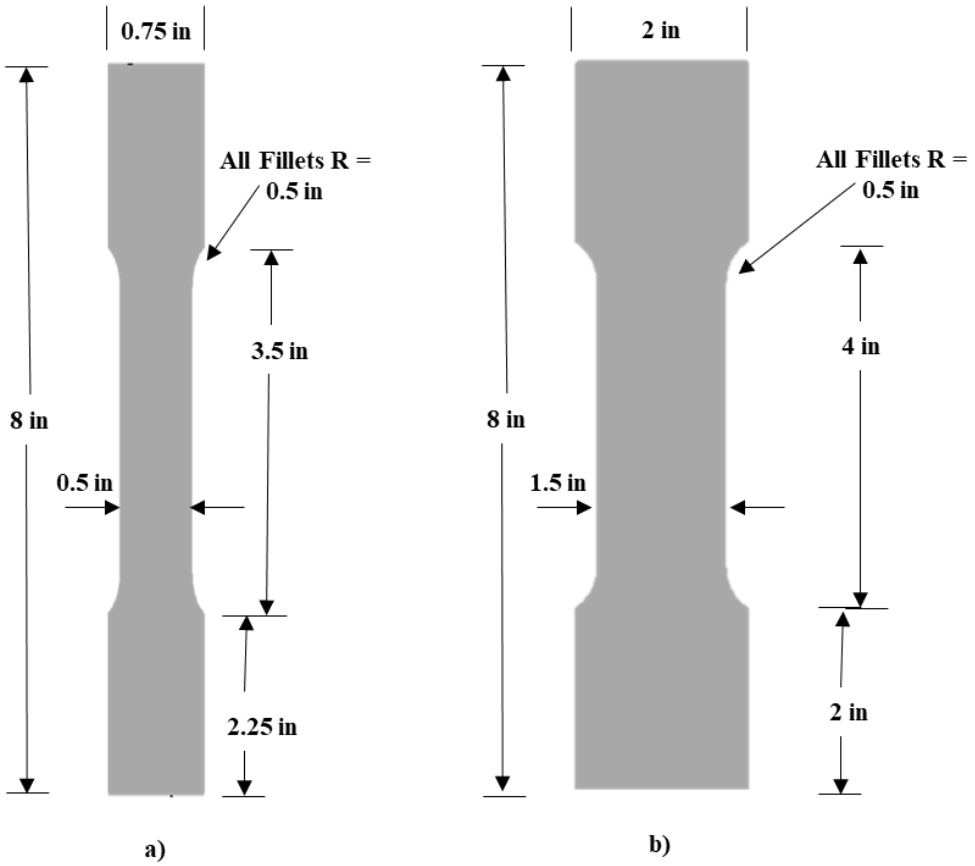

Figure 3. The sample geometries of both the 50CR and reduced area weld tension samples for a) Group 1 samples and b) Group 2 samples

Full-size weld CVN samples were machined from Group 1 plates in the TL orientation and tested on a calibrated 300 ft·lbf capacity Charpy testing machine in accordance with ASTM E23.[47] The number of samples tested at -20°F and the additional test temperatures explored is presented in Table 3. In summary, five to ten samples were tested at -20°F and two to three samples were tested at each of the following temperatures: -100, -60, -30, -10, 10, 40, 70, and 150 °F. Testing temperatures below room temperature were achieved using an ethanol bath in accordance to ASTM E23.[47] Testing at 150 °F was achieved by heating the samples in hot water and used to determine an upper shelf impact energy. Analysis of the DBTT behaviors involved least squares minimization to obtain a best-fit double hyperbolic tangent curve. The resulting curve is commonly used to define three-regimes: the upper shelf, transition region, and lower shelf. Finally, five full-size welded CVN samples were machined from each Group 3 plate and tested in accordance to AWS D1.5 Section 5.19.5.[41]

Table 3. List of welding parameter combinations used in the study, along with the number of specimens tested at -20 °F and additional temperatures at which 2 or 3 samples were tested

Welding Parameter Combination	Number of samples tested at -20°F	Additional Test Temperatures
309L, 50 kJ/in, 300 °F	10	n/a
309L, 75 kJ/in, 125 °F	10	n/a
309L, 75 kJ/in, 300 °F	10	n/a
309L, 75 kJ/in, 450 °F	10	-100°F, -60°F, -30°F, -10°F, 10°F, 40°F, 70°F, and 150 °F
309LC, 50 kJ/in, 300 °F	10	n/a
309LC, 75 kJ/in, 125 °F	10	n/a
309LC, 75 kJ/in, 300 °F	10	n/a
309LC, 75 kJ/in, 450 °F	10	-100°F, -60°F, -30°F, -10°F, 10°F, 40°F, 70°F, and 150 °F
309LSi, 75 kJ/in, 125 °F	5	n/a
309LSi, 75 kJ/in, 450 °F	5	-100°F, -60°F, -30°F, -10°F, 10°F, 40°F, 70°F, and 150 °F
316L, 75 kJ/in, 125 °F	5	n/a
316L, 75 kJ/in, 450 °F	5	-100°F, -60°F, -30°F, -10°F, 10°F, 40°F, 70°F, and 150 °F

Side-Bend Testing

Four side-bend test samples were machined from each Group 3 plate and tested in accordance to AWS D1.5 Section 5.19.2.[41]

Fractography

Fractography was performed on the 1/2 in thick 50CR CVN samples tested at the highest and lowest temperatures using OM. Similarly, OM was used to characterize the Group 1 CVN samples welded using a heat input of 75 kJ/in and a maximum interpass temperatures 450 °F at the highest, lowest, and AWS D1.5 testing temperatures. The conclusions made from the OM were then confirmed using SEM.

RESULTS AND DISCUSSION

At the time of the project initiation, the 309L, 309LSi, and 316L used in this study did not meet the Buy America requirements for FHWA funded projects.[49] However, a metal-cored wire, 309LC, met the regulation. Although the Buy America regulations were not a primary concern for this project, they were taken into consideration for the project recommendations and future implementation. Micrographs of the two different wire types (solid and cored wire) can be seen in Figure 4. The 309LC metal-cored wire consisted of a metallic sheath mechanically wrapped around a mixture of metal powders. EDS mapping of the cored wire, shown in Figure 4c-f, revealed that the metal powder primarily consists of pure nickel (Ni) particles and particles of a 70% chromium (Cr), 28% iron (Fe) alloy containing trace amounts of manganese (Mn), and silicon (Si). The metallic sheath had a nominal composition of 68% Fe, 19% Cr, 9% Ni, 1.5% Mn, and 1% Si (wt%). Table 4 provides a compositional analysis of solid filler wires using EDS.

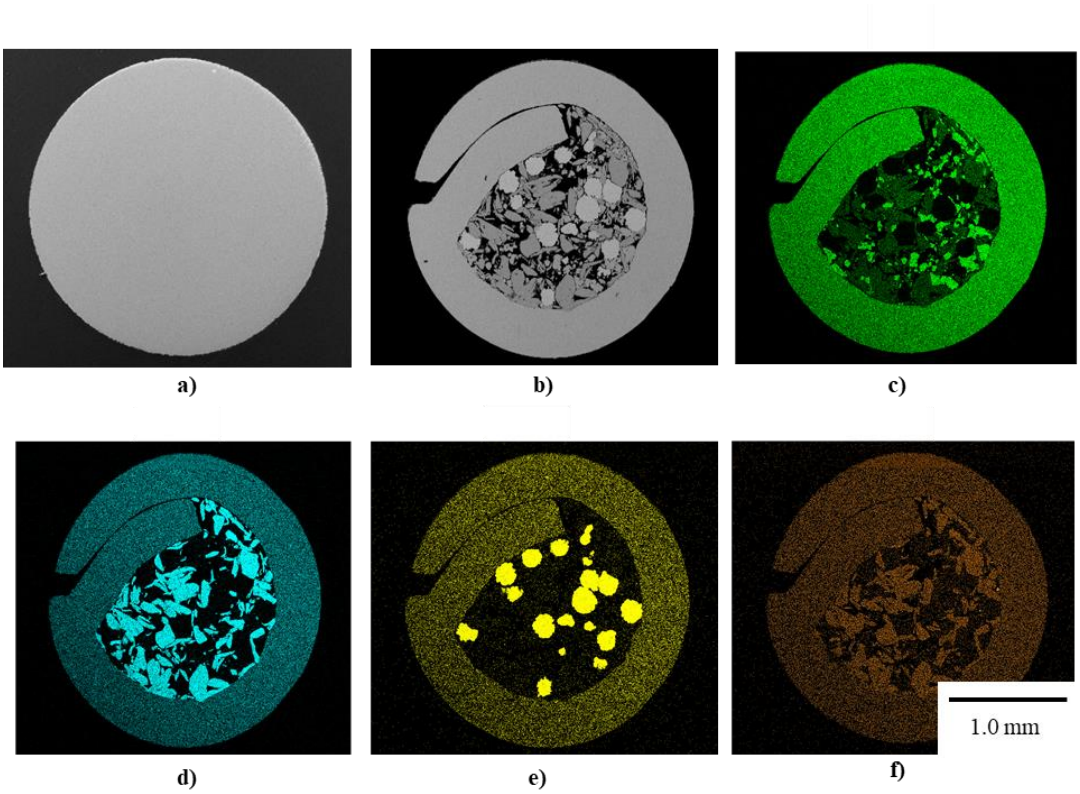

Figure 4. Representative SEM micrographs of a) solid wire and b) cored wire samples. EDS composition maps were performed on the 309LC cored wire samples, c) Fe, d) Cr, e) Ni, and f) Mn showing the compositional makeup of the powder core sample. Note, the color overlays represent the intensity or quantity of the element being identified. Image d, showing Cr, indicates that the particles inside the sheath is rich in Cr when compared to the sheath, and when image d is compared to image f, showing Mn the cored wire is not as rich in Mn. Similar to image d, image e, showing Ni, follows the same trend when comparing the particles inside the sheath to the sheath, and the Mn composition that is shown in image f. SEM = scanning electron microscope and EDS = energy dispersive spectroscopy

Table 4. Semi-quantitative compositional analysis of solid filler wires using EDS

Filler Wire	C	Cr	Ni	Mo	Mn	Si	P	S	Cu
ER309L[48,49]	0.03	23.0 – 25.0	12.0 – 14.0	0.75	1.0 – 2.5	0.30 – 0.65	0.03	0.03	0.75
EDS 309L		24.6	13.1		1.6	0.4			
ER309LSi[48]	0.03	23.0 – 25.0	12.0 – 14.0	0.75	1.0 – 2.5	0.65 – 1.00	0.03	0.03	0.75
EDS 309LSi		24.4	13.5		2.3	0.8			
ER316L[48]	0.03	18.0 – 20.0	11.0 – 14.0	2.0 – 3.0	1.0 – 2.5	0.30 – 0.65	0.03	0.03	0.75
EDS 316L		19.5	11.8	2.1	2.1	0.4			

Note: C = carbon, Cr = chromium, Ni = nickel, Mo = molybdenum, Mn = manganese, Si = Silicon, P = phosphorus, S = sulfur, Cu = copper, and EDS = energy dispersive spectroscopy

Welded Plate Fabrication

Group 1 and 2 plates were welded using the joint preparation indicated by AASTO/AWS D1.5 SAW B-U3c-S.[41] All but one of the Group 1 plates passed visual inspection and radiographic testing in accordance with AWS D1.5 Section 6C, which states that welded plate should be free of any cracking or visible piping porosity, limited internal porosity, and have thorough fusion between adjacent weld layers, and between the weld metal and the base plate.[41] It was noted that one of the welded plates (which used 309LC filler wire, at a heat input of 75

kJ/in, and a maximum interpass temperature of 300 °F) contained a 5/64 in (2 mm) weld gap, which was determined to be due to welding defect. Mechanical testing of this welded plate was still performed to determine if it would still meet the mechanical property requirements. Those results are not included within the main body of this report, but are included in Appendix B.

The Group 3 plates were welded using the AWS D1.5 SAW B-U2-s joint configuration.[41] A comparison of the welding parameters utilized on the PQR plates is presented in Table 5. A lower heat input was used for both the root and cap weld passes, but they are not included in the heat input calculation per AWS D1.5.[41] Fewer passes were required for the 309LC filler wire because it has a higher overall deposition rate and lower fume and spatter.[50-54] Visual, radiographic, and ultrasonic inspection were performed on both PQR plates in accordance to AWS D1.5[41] and no defects were reported.

Finally, it was noted that the wire feed speed employed for the cored wire was reported by the girder fabricator to be 53% faster than that of the solid wire (275 vs. 180 inches per minute) for the welding of the 1/2 in thick plates in Group 1. Welding of the PQR plates (Group 3) with cored wire was performed with wire feed speeds, which were 31% faster than the solid filler wire (225 vs. 172 inches per minute). This is necessary because the cored wire has a lower mass density, due to its construction incorporating powder, as shown in Figure 4.[51,52,53]

Table 5. Welding parameter data provided by girder fabricators for welding of Group 3 plates

Welding Parameter	309L, 90 kJ/in, 450 °F	309LC, 90 kJ/in, 450 °F
Total Number of Weld Passes	12	10
Average Heat Input (kJ/in)	88.3	88.1
Average Current (A)	566	514
Average Voltage (V)	39	40
Average Travel Speed (in/min)	15	14
Average Feed Speed (in/min)	172	225

Compositional Analysis

A comparison between the nominal composition and that of the current study are shown in Table 6. The single values given in the first two rows of the table indicate a maximum weight percentage (wt%) of the element allowed in the alloy. Although Mo is not included in the compositional requirements for 50CR according to ASTM A709[48], ASTM A751[55] allows for the addition of alloying elements not specified as long as the steel can still fulfill the necessary mechanical properties, which in this case are 50 ksi for yield strength, 70 ksi for tensile strength, and 21% elongation.

Table 6. Comparison between the ASTM A709 grade 50CR requirements, the 50CR producers' nominal composition, and the composition of the 50CR used for the study.

Alloy	C	Mn	P	S	Si	Cr	Ni	N	Mo	Cu	Al
ASTM[48]	0.030	1.50	0.040	0.010	1.00	11.2 – 12.5	1.50	0.030			
Duracorr[16]	0.025	1.50	0.040	0.010	0.70	11.0 – 12.5	1.00	0.030	0.20 – 0.35		
Current Study	0.01	1.23	0.025	0.004	0.36	11.40	0.36	0.008	0.28	0.10	0.004

Note: C = carbon, Mn = manganese, P = phosphorus, S = sulfur, Si = Silicon, Cr = chromium, Ni = nickel, N = nitrogen, Mo = molybdenum, Cu = copper, Al = aluminum

A prediction of the fusion zone phase content can be made by plotting the Cr_{eq} and Ni_{eq} compositions of the filler metal on a Schaeffler diagram (Figure 5). By connecting these compositions with that of the base material (50CR) a dilution line is revealed. For this study, the dilution line includes regions with (a) austenite and ferrite (little dilution), (b) a combination of austenite, ferrite, and martensite, or (c) martensite and ferrite (in cases of extreme dilution). The compositions of the fusion zones determined by EDS were found to be uniform throughout the welds, and using the data from those area scans, the dilution of Cr and Ni by the base metal was estimated to be 30 - 60% for solid wire and 20 – 50% for the metal cored wire. The ranges of measured compositions (by EDS) are depicted by ellipses in Figure 5. These values of dilution are consistent with available literature on submerged arc welding dilution, and place all of the welds squarely within the region of the Schaeffler diagram, which predicts a combination of austenite, ferrite, and martensite.[2-4,31] In particular, the predicted ferrite concentrations are in the range of 20-30%.[29,30,31] This prediction also means that the solidification mode for all of the fusion zones will involve the formation of primary δ-ferrite, which will then undergo a solid-state transformation to austenite (termed the F solidification pathway in the introduction).[31,33] The relatively slow cooling rates experienced by the welds is offered as an explanation for the absence of martensite.

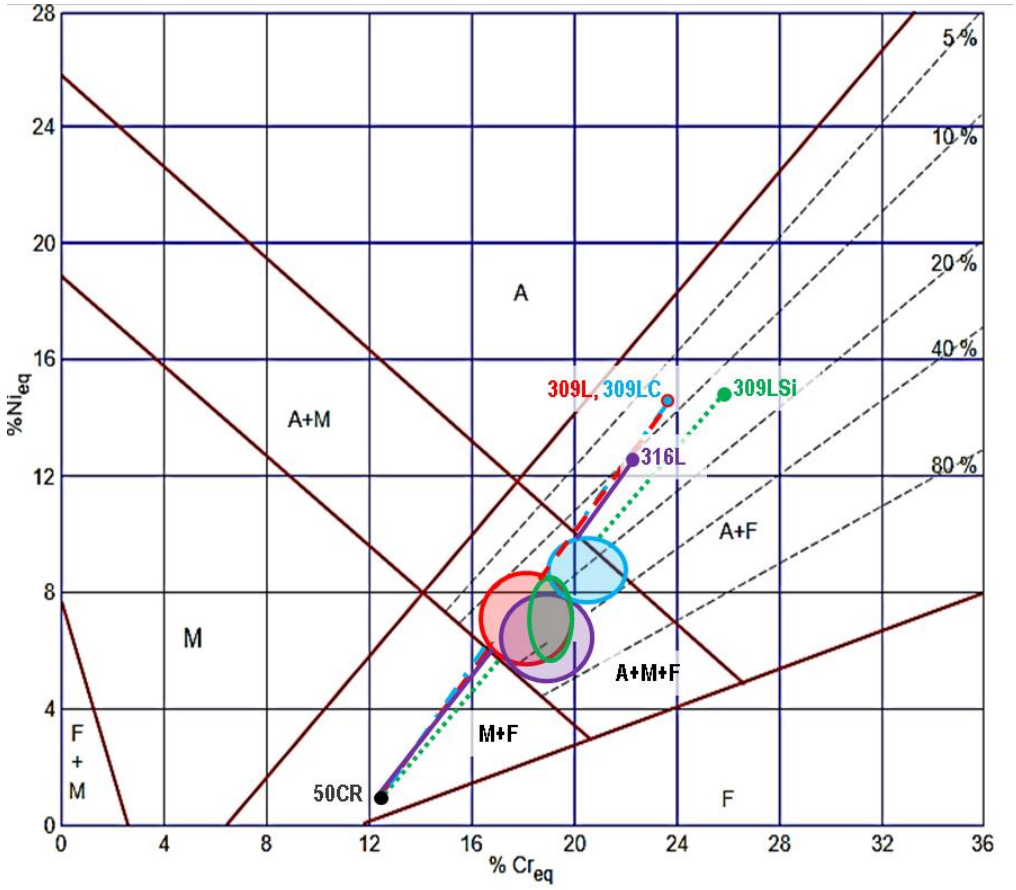

Figure 5. Schaeffler diagram (after reference 31) including the compositions of the filler wires used in this study, dilution lines, and the ranges of measured compositions (by EDS) depicted by ellipses of the 309L (red), 309LSi (green), 309LC (blue), and 316L (purple) plotted as ellipses which fall squarely in the region labeled *A+M+F* (austenite + martensite + ferrite). EDS = energy dispersive spectroscopy

Microstructural Analysis

Conventional Metallography

Micrographs of 50CR base metal revealed the expected[1,2,16] dual-phase microstructure for this type of alloy and product form (see Figures 6 & 7). The microstructure is comprised of elongated ferrite grains between bands of tempered martensite grains, which ranged from 5 to 50 microns in thickness. The phase identification was determined by the color contrast in the micrographs. Vilella's etchant reveals general features of the microstructure (such as grain size and shape) and darkens the martensite grains more than the ferrite (see Figure 6).[1,4] The dark regions in the optical micrographs (which are highlighted with yellow circles) reveal the presence of stringers as well as isolated particles of intermetallic particles, which were found to contain Al or Si based according to the semi-quantitative EDS shown in Figure 6d). Sometimes these stringer particles also contained trace amounts of Mg, Ca, and Ti. Optical micrographs obtained at 250x magnification were processed using an image analysis program, which thresholded the micrographs such that the ferrite appears white and the martensite appears black. Analysis of such micrographs revealed a ferrite content of 5 to 15 volume % (vol%) in the 1/2 in

plates and 5 to 10 vol% in the 1 in plates, with the remainder determined to be martensite. One key difference between the 1/2 in and 1 in plate microstructures is the lower degree of alignment of the ferrite microstructure, which is less pronounced in the latter (see Figure 7).

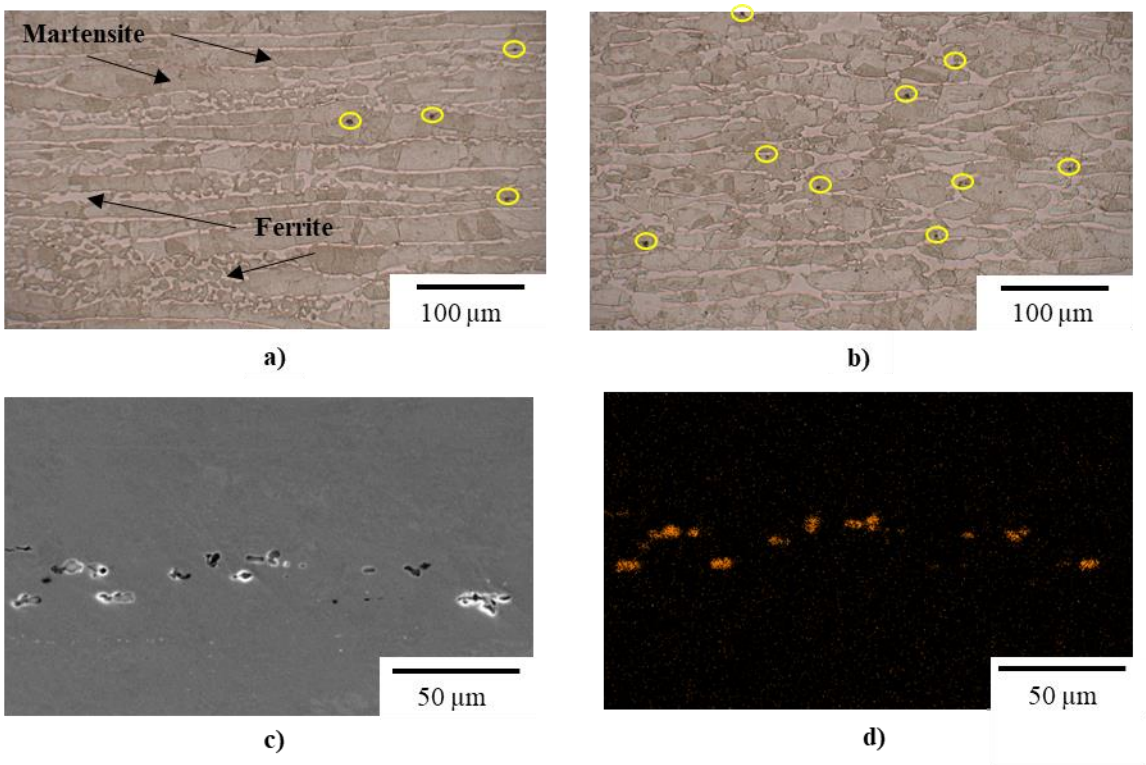

Figure 6. 50CR microstructure taken from the longitudinal face of 1/2 in thick base plate at 600x magnification using bright field OM (aluminum containing particles highlighted with yellow circles around each particle) in a) longitudinal and b) transverse planes; c) SEM micrograph of stringers; d) EDS map showing the presence of aluminum. OM = optical microscopy, SEM = scanning electron microscope, and EDS = energy dispersive spectroscopy

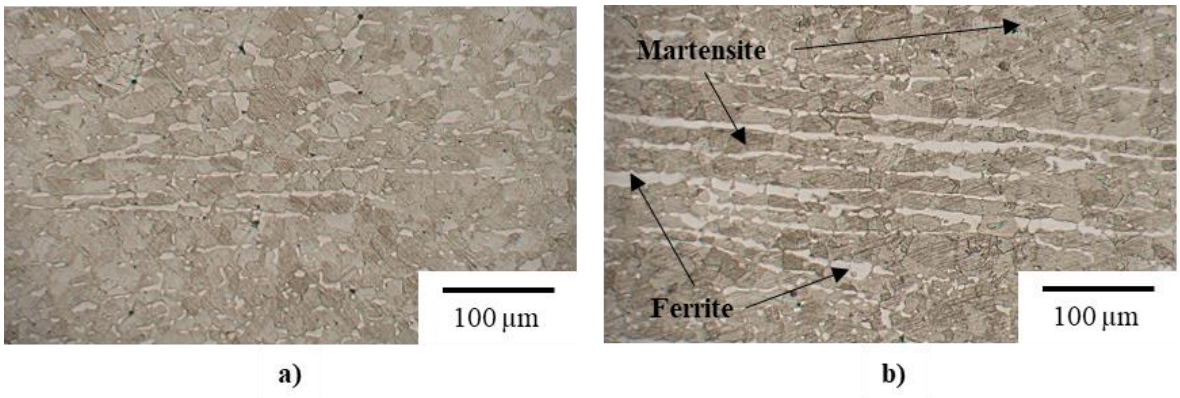

Figure 7. 50CR microstructure taken from the longitudinal face of 1 in thick base plate at 600X magnification using bright field optical microscopy. Vilella's reagent colors martensite and leaves ferrite unetched.

Microstructural analysis of both Group 1 and 2 welded samples revealed four distinct microstructural zones. These four zones are the fusion zone, the coarse-grained or high temperature heat affected zone (coarse or HT-HAZ), the fine-grained or low temperature heat

affected zone (fine or LT-HAZ), and the unaffected base material, shown in Figure 8. This is consistent with previous research performed on 50CR[24] and its legacy alloy, 3CR12.[8,56] Image processing of the fine LT-HAZ revealed that the ferrite content remained at ~10 vol%, and the size of the martensite bands remained at 5 to 50 microns. Metallographic analysis of the fusion zones revealed various particles with sizes up to tens of micrometers. EDS revealed that these particles were commonly Al-Mn-Si oxides. These particles were of varying size and no correlation with filler wire, heat input, or maximum interpass temperature was observed.

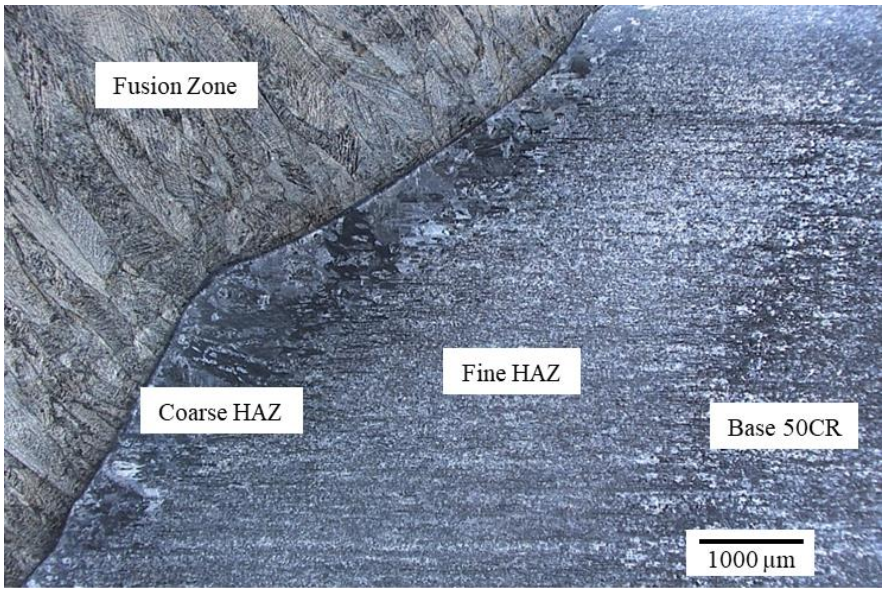

Figure 8. Typical welded plate microstructure for all of the filler wires, taken using 35X magnification and dark field optical microscopy. HAZ = heat affected zone.

Austenitic filler wires are designed to have at least 5 vol% residual δ-ferrite to prevent hot cracking of the austenitic weld.[27] No cracking of any sort was found in the welded plates in the present study. Kalling's No.2 etchant, which preferentially attacks ferrite more readily than austenite[45], and image analysis software was able to differentiate between the two phases (again enabling thresholding of the image, this time coloring ferrite black and austenite white in the binary 2D image). Based on a two-sided T-test, it can be stated with 95% confidence that neither raising the heat input nor the maximum interpass temperature causes a statistically significant change in the amount of residual δ-ferrite in the fusion zone in the Group 1 plates for all four filler wires tested. The nominal ferrite content in the fusion zones is presented in Table 7. The rank order in ferrite content is the same for the two plate thicknesses: 316L < 309L = 309LSi < 309LC, all of which are higher than the minimum δ-ferrite (5 vol%) required. Full reporting of the results obtained in this study are presented in Appendix C.

Table 7. Average ferrite content (in volume %) in the fusion zone for plate groups 1 and 2

Weld Filler Wire	316L	309L	309LSi	309LC
Group 1 (1/2 in)	10	12	12	17
Group 2 (1 in)	15	18	18	26

The three macro-etches from each PQR test plate were found to be acceptable. The weld fusion zone was free of cracks and porosity, and there was thorough fusion between adjacent

layers of weld metal as well as between the weld metal and the base material. That said, there is a subtle trend in the microstructure, which will be shown to correlate with the ductile to brittle transition temperature (DBTT) of the resulting welds. Figure 9 reveals that welds produced in plates of 1/2 in thickness using the metal-cored wire (309LC) have a somewhat finer, and less aligned macrostructure, as compared to the welds produced using conventional 316L (a) and 309L (b). Higher magnification images in Figure 10 further emphasize the fact that the cored wire induces a finer microstructure in the fusion zone. The images illustrate that use of the cored wire results in a finer structure, both at the level of the columnar prior δ-phase grains (Figure 9) and in the fineness of the Widmanstätten structure of the austenite phase that results from a solid-state phase transformation (Figure 10).

X-ray Diffraction

Conventional powder XRD revealed that there was no residual face centered cubic (FCC) γ-austenite (above the minimum detection limit) in the microstructure of the 50CR base material. The XRD pattern of 50CR, shown in Figure 11a, revealed only body centered cubic (BCC) peaks indicative of both ferrite and martensite (which cannot be discriminated in such powder diffraction experiments). Both FCC γ-austenite and BCC δ-ferrite were revealed to be present in the fusion zone, as shown in Figure 11b. As mentioned above, austenitic filler wires are designed to retain at least 5 vol% δ-ferrite, to prevent solidification cracking. The larger δ-ferrite (BCC_{110}) peak in the diffraction pattern of the weld produced using 309LC confirms that it results in the retention of a higher volume fraction of ferrite, as compared to conventional solid 309L filler wire (Figure 12b). Again, the range of retained ferrite observed in this study is considered to be in the safe range, where no correlation between ferrite content and ductility has been observed. Only at very low < 2 vol% is there a correlation with hot cracking[57] and at very high > 50 vol% is there a correlation with low temperature embrittlement.[37]

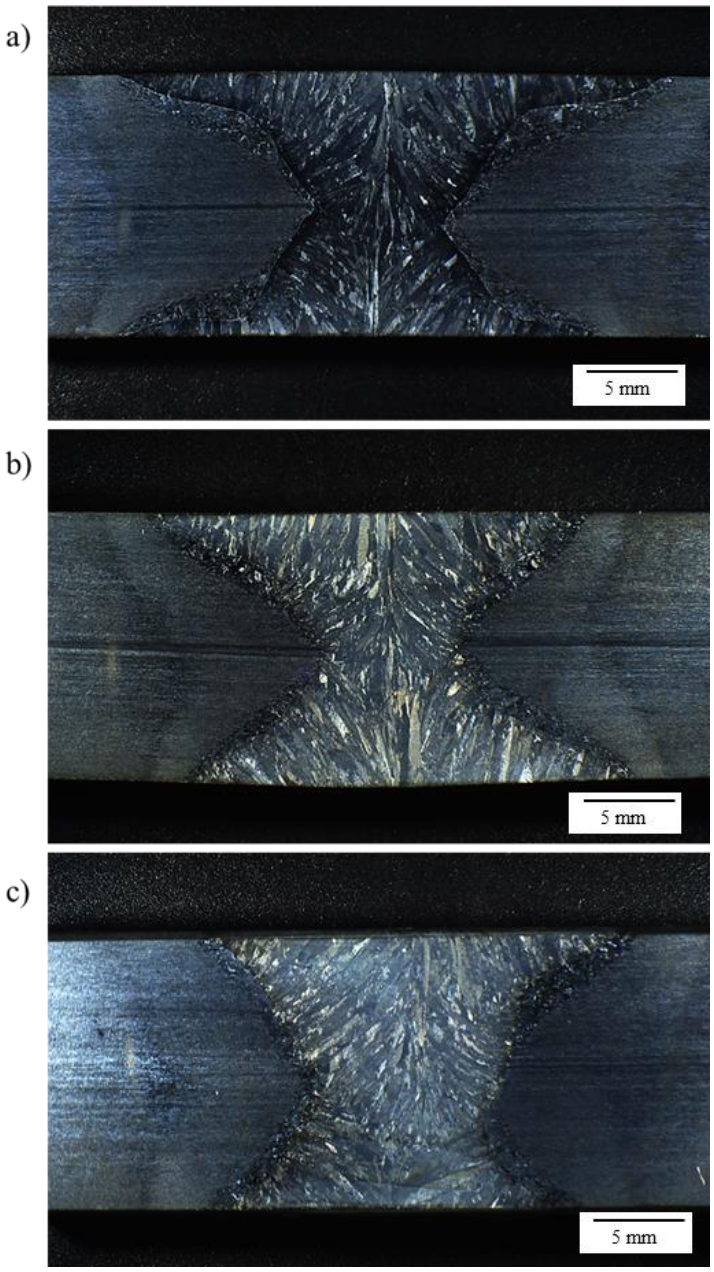

Figure 9. Representative macro etch images of the fusion zone from welds produced using a) 316L, b) 309L, and c) 309LC which illustrates a more irregular microstructure along the centerline of the weld in case (c), as compared with the large, aligned grains in cases (a) & (b).

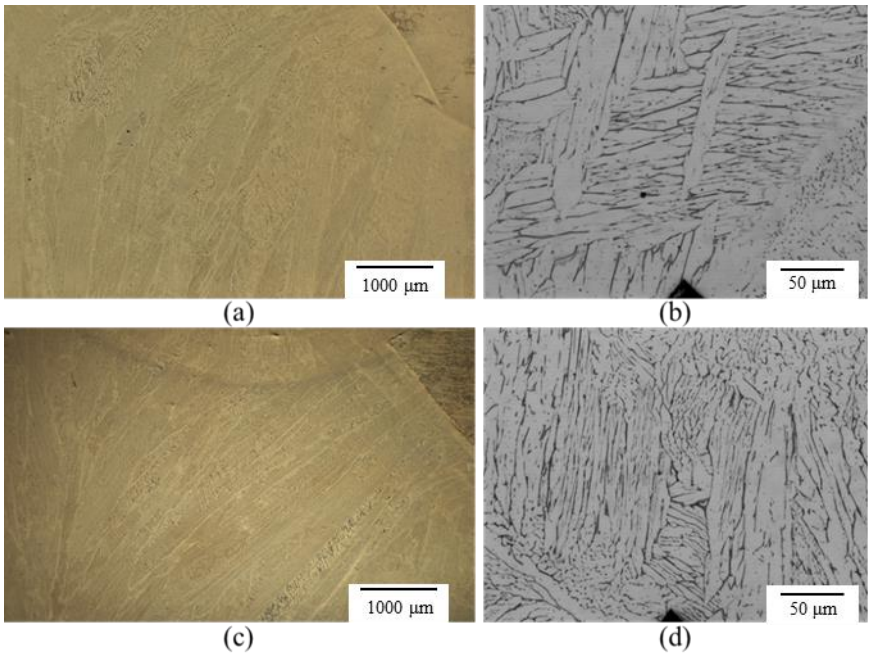

Figure 10. Representative microstructural images of the fusion zones of welds in 1/2 in plates using 309L (a & b) and 309LC (c & d) filler metals with a heat input of 75 kJ/in and an interpass temperature of 125 °F (a & c) and 450 °F (c & d). The images illustrate that use of the cored wire results in a finer structure, both at the level of the columnar prior δ-phase grains (a & c) and in the fineness of the Widmanstätten structure of the austenite phase which results from solid state phase transformation (b & d)

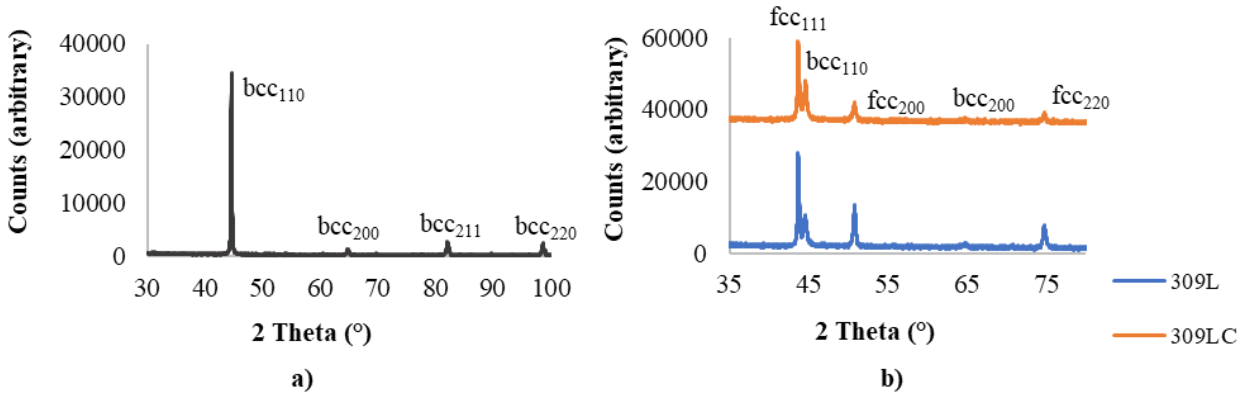

Figure 11. XRD pattern of a) the base 50CR is comprised entirely of BCC peaks with no retained austenite (FCC) and b) the fusion zone of Group 3 plates having peaks from both austenite and retained δ-ferrite

Mechanical Testing

Hardness Testing

Microhardness testing of the 50CR base metal revealed an average hardness of 200 ± 10 HV, for Groups 1 (1/2 in) and 2 (1 in). The hardness of the 1 in thick Group 3 plates was determined to be slightly higher at 245 ± 10. These differences in hardness between the groups reflect the variability of the as-received based material.

Microhardness data taken from welded samples of Group 1 all reveal enhanced hardness within the weld. The higher hardness in the HAZ region of all the welds is due to precipitation of carbides.[10,58] Figure 12 reveals an interesting distinction between the plates welded with 75 kJ/in heat input and 450 °F interpass temperature using the solid filler wires (309L, 309LSi, and 316L) and the metal cored wire (309LC). The plates welded with a solid filler wire had the highest hardness values (ranging from 300 – 350 HV) in the fusion zone, and a narrow region of depressed hardness right outside the fusion zone. On the other hand, the hardness of the fusion zone resulting from the use of 309LC was only about 200 HV, similar to that of the base metal. The highest hardness values in the 309LC samples, which ranged from 250 – 300 HV, were located in the fine HAZ (not in the fusion zone).

Based on the micro-hardness results on the Group 1 samples welded using a maximum interpass temperature of 300 °F, it was clear that these samples had been welded with more passes than the other samples. Although this was not originally planned for and occurred due to welder variability, this represents a welded plate that has been repaired due to a detected weld flaw. The highest hardness found in these samples was approximately 400 HV. Typical microhardness values for the Group 2 samples were in the range of 300 – 375 HV, consistent with the fine HAZ hardness values of Group 1 plates welded using a maximum interpass temperature of 300 °F.

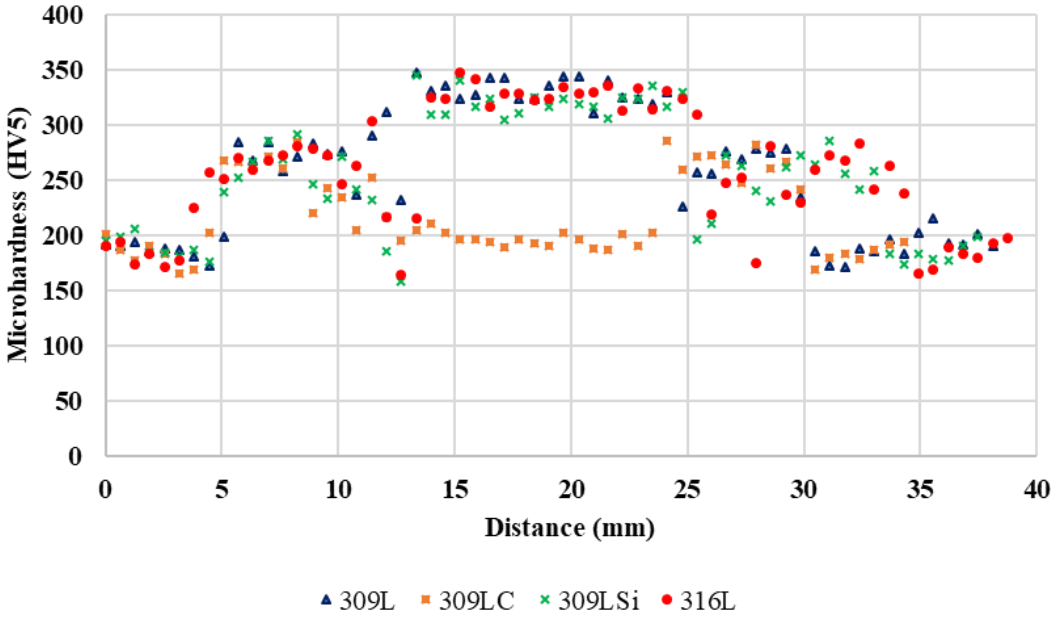

Figure 12. Typical hardness trends found in across the second weld pass using the different fillers, 75 kJ/in, and 450 °F in the Group 1 plates.

Tensile Testing

The base 50CR material from 1/2 in thick plates examined in this study surpassed the minimum requirements for the tensile properties indicated in ASTM A709, a yield strength of 50 ksi and a tensile strength of 70 ksi, and an elongation of 21% for plates less than 24 in in width and 19% for plates wider than 24 in as shown in Table 7.[45-48] In a prior study of 3Cr12, it was

observed that the plates are prone to delamination-type failure, where secondary cracks run parallel to the plane of the plate.[8] This observation suggests that 3Cr12 and similar alloys such as 50CR may be susceptible to lamellar cracking during fillet welding of T-joints typical of welded plate girders and for which the Cranfield test was developed.[59] However, Grobler investigated this possibility and, yet, did not observe lamellar cracking in his study of 3CR12.[8] However, Grobler still indicated that it is an issue worthy of further consideration and suggests a means of exploring it. Whether or not this possible failure mode would affect the performance of 50CR structural members is beyond the scope of the current report. Notably, the present investigation of butt-joints revealed no cracks of any sort in the as-welded plates.

In order to explore the change in the mechanical properties of the welded plate as heat input and maximum interpass temperature were increased; tensile testing was performed on each of the Group 1 and 2 plates. Because 50CR is not yet included in AWS/D1.5 there are no tensile requirements for welded 50CR, so the data was compared to 50CR base metal requirement set forth by ASTM A709.[45-48] Ten samples were tested from each of the plates welded using the 309L and 309LC filler wires, and five samples were tested from each of the plates welded using 309LSi and 316L for Group 1. Three reduced tension samples were tested for each of the Group 2 plates. A complete reporting of all data obtained is presented in Appendix D and is summarized below in Table 8.

Table 8. Tensile properties of 1/2 in thick ASTM A709 50CR used for study

Sample Direction	Yield Strength (ksi)	Tensile Strength (ksi)	% Elongation
Longitudinal	66-68	83-90	28.3 - 28.9 %
Transverse	64-67	81-87	30.2 - 31.1 %

Based on the results from one-sided t-testing of data obtained from mechanical testing of 1/2 in welded plates in Group 1, it can be said with at least 95% confidence that a sample selected at random from any of the welding combinations explored will surpass the minimum yield strength requirement of 50 ksi dictated by ASTM A709 for grade 50CR.[48] This can be said regardless of which filler wire, heat input (50 kJ/in and 75 kJ/in), and maximum interpass temperature (125 °F to 450 °F) were employed. Based on the two-sided t-test, it can also be said with 95% confidence that neither increasing the heat input nor increasing the maximum interpass temperature caused a statistically significant change to the yield strength for all consumables. This can be said even though different numbers of welding passes were used to weld the plates with a heat input of 75 kJ/in and a maximum interpass temperature of 300 °F.

Using the same statistical analysis procedure as was used for the yield strength data, it can be said with at least 95% confidence that a 1/2 in welded plate sample selected at random will meet the 70 ksi tensile strength minimum requirement set forth by ASTM A709[48], regardless of the alloy of weld wire employed in this study. It can also be stated with a high level of confidence that neither increasing the heat input, nor increasing the maximum interpass temperature caused a statistically significant change in the tensile strength.

ASTM A709, which is currently used as the standard to which welded 50CR's mechanical properties are compared, contains minimum requirements for yield strength, tensile strength, and percent elongation.[48] In this study, the fracture typically occurred outside of the reportable region specified in the standard. Indeed, only 14% of the all of the welded samples

fracturing within the reportable region. This is due to the fact that the weld nugget was stronger than the base material, causing the strain to localize in the surrounding, unaffected 50CR based material, where the fracture ultimately occurred.

Tensile test data from the 1 in thick Group 2 plates was also compared to the minimum requirements dictated by ASTM A709.[48] The average values from the three tensile tests all met the minimum requirements for both the yield strength and the tensile strength. A lower level of confidence level (< 90%) associated with the yield strength of the Group 2 samples is due to the smaller number of samples tested. One-sided t-tests of the tensile strength data showed with at least 95% confidence that a sample selected at random from all of the welding parameter combinations will meet the 70 ksi required minimum.[48] Tensile testing on the two Group 3 welded PQR plates included two reduced section tensile samples and one all weld metal tensile bar. The data obtained from this testing is listed in Table 9. The tensile strengths for the reduced section samples exceed the minimum tensile strength requirement of 70 ksi and the yield strength exceeded the minimum requirement of 50 ksi.[48] The tensile testing data from the two PQR plates showed comparable results when compared to the data from analogous plates from Group 2.

Table 9. Results from testing of Group 3 plates welded using 309L and 309LC with a heat input of 90 kJ/in and a maximum interpass temperature of 450 °F.

Sample Type	Yield Strength (ksi)	Tensile Strength (ksi)	Elongation (%)	Reduction in Area (%)
309L reduced section	59.5 (56, 63)	89.5 (89, 90)	24.5 (23, 26)	25 (25, 25)
309L all weld	54	88	30	27
309LC reduced section	58 (61, 55)	93.5 (95, 92)	37 (42, 32)	34.5 (36, 33)
309LC all weld	58	94	36	46

Note: Data in parenthesis represents the actual data from the PQR plates.

CVN Testing

Because Virginia is in temperature zone 2, as defined by AASHTO LRFD Bridge Design Specifications, three base plate samples were tested in each orientation at 40 °F[48,60] The 50CR samples surpassed the minimum impact energy requirements dictated by ASTM A709 in both orientations.[48] The LT samples showed higher energy absorption than the TL samples, which is supported by previous work.[61] In fact, the LT sample tested at 10 °F stopped the hammer with an impact energy of 298 ft·lbf. To prevent damage to the Charpy testing machine due to operation within 80% of its maximum capacity, no additional LT samples were tested at 10 °F or above.[47] The three TL samples had impact energies of 215, 164, and 161 ft·lbf, averaging to 180 ft·lbf at 40 °F, which falls within the range of the data previously.[1,23,60] These values greatly exceed the 15 ft·lbf minimum required for grade 50CR structural steel.[48] Figure 13 shows the measured impact energy as a function of temperature for the LT and TL 50CR samples, with additional test temperatures chosen to fill out the transition temperature curve. The DBTT was determined to be -38 °F in the LT orientation and -40°F in the TL orientation.

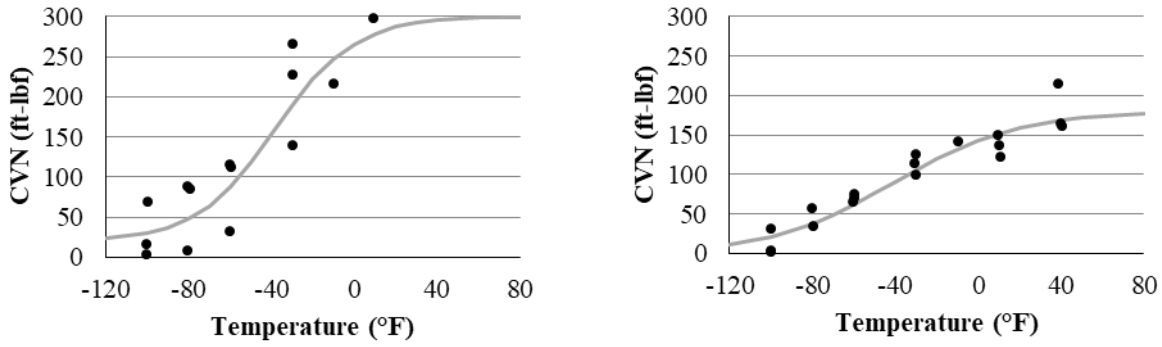

Figure 13. Charpy impact data for the base plate, 50CR, for the entire range of temperatures tested (a) LT sample orientation and (b) TL sample orientation. The length of the LT sample is oriented in the longitudinal (L) direction and the V notch (cracking direction) is parallel to the transverse (T) direction. The TL sample is oriented in transverse (T) direction and the V notch (cracking direction) is parallel to the longitudinal (L) direction. This is shown in Figure 1.

For 50W, non-fracture critical members, the specified testing temperature for AASHTO zones 1 and 2 is 0 °F and -20 °F for zone 3.[41] For fracture critical components, the testing is to be performed at -20 °F, regardless of zone.[41] The requirement for fracture critical welds is 25 ft-lbf, however there are currently no requirements for 50CR. A complete listing of data obtained is presented in Appendix E, and a summary of the results is provided below.

The data obtained from the Group 1 plate is shown in Table 10. Within the first set of samples, it can be seen that the first set of five samples welded using 309L filler, at a heat input of 75 kJ/in and a maximum interpass temperature of 450 °F, failed to pass the standard. A second set of five samples passed, indicating that this condition is a borderline case. Two-sided t-tests indicate with 95% confidence that increasing the maximum interpass temperature did not have a significant effect on the CVN values, in comparison to the heat input. Increasing the heat input from 50 to 75 kJ/in resulted in a 29% decrease in CVN impact energy (from an average of 53 to 38 ft·lbf).

Table 10. Average impact energies of the Group 1 full-size CVN samples

Filler Wire	Heat Input (kJ/in)	Maximum Interpass Temp. (°F)	Average CVN (all 5 samples, ft·lbf)	AWS D1.5 CVN (ft·lbf)**
309L	50	300	53	53
309L	75	125	21	20
309L	75	300	38	39
309L	75	450	17*	17*
309L Retest	75	450	22	21
309LC	50	300	57	57
309LC	75	125	40	39
309LC	75	450	41	41
309LC Retest	75	450	39	36
309LSi	75	125	26	26
309LSi	75	450	20	20
316L	75	125	24	24
316L	75	450	25	25

Note: * failed to meet minimum CVN requirements of the AWS D1.5
****AWS D1.5 indicates the average of five samples with the highest and lowest test values thrown out should be reported**[41]

The CVN impact energies for Group 2 plate samples measured as a function of the heat input and maximum interpass temperature are presented in Table 11. They all greatly exceeded the AWS D1.5 minimum requirement for both fracture and non-fracture critical components.[41] One-sided t-testing of the tensile strength data showed with at least 95% confidence that a sample selected at random from all of the welding parameter combinations will exceed the requirement. The results of the present study agree with previous testing of welded 50CR plates performed by Oregon using only 309L filler wires.[23]

Table 11. Average impact energies of the Group 2 full-size CVN samples

Filler Wire	Heat Input (kJ/in)	Maximum Interpass Temp. (°F)	CVN All 5 Samples (ft·lbf)	AWS D1.5 CVN (ft·lbf)
309L	70	300	72	74
309L	90	300	66	65
309L	90	450	50	50
309LC	70	300	74	74
309LC	90	300	71	71
309LC	90	450	71	71
309LSi	70	300	78	78
309LSi	90	300	73	74
309LSi	90	450	74	75
316L	70	300	43	43
316L	90	300	52	49
316L	90	450	65	69

One set of five CVN samples, with the notch placed in the weld, were tested for each PQR plate each yielding higher values than Group 1 but comparable to those from Group 2, as shown in Table 12. In the Group 1 plate, full-sized CVN samples were taken from the middle 3/8 in of the 1/2 in thick plate. For the Group 2 and 3 plates, full-size CVN plates were also taken from the middle 3/8 in of the plate, keeping in mind that there are more weld passes used when welding these plates.

Table 12. Summary of impact energies of PQR full-size weld samples

Filler Wire	Heat Input (kJ/in)	Maximum Interpass Temperature (°F)	CVN All 5 Samples (ft·lbf)	AWS D1.5 CVN (ft·lbf)
309L	90	450	90	89
309LC	90	450	93	93

A ductile to brittle transition (DBT), typically manifesting as a rapid drop in the impact energy as a function of temperature, is typical in BCC materials (in the case of steel, the ferrite and martensite phases), but not in FCC materials (the austenite phase). This is due to a more temperature- and rate-sensitive yield strength in the BCC phases.[63] Previous research on duplex stainless steels (50-50 vol% ferrite and austenite) reports a three-regime transition temperature curve, similar to that of purely ferritic steels.[64] The temperature transition curves of the four filler wires welded using a heat input of 75 kJ/in and a maximum interpass temperature of 450 °F on the Group 1 plates, deemed the most aggressive welding parameter combination, are shown in Figure 14.

Based on the results, the three-regime transition curve was abandoned in favor of linear fitting which is more consistent with a microstructure predominantly containing austenite.[65] The impact energies for the plates welded using 309LC were consistently higher in comparison to those welded with the three solid filler wires. Based on the fitted transition temperature curve, 50CR welded using 309LC will not fall below the 20 ft·lbf minimum until well below -100 °F, significantly lower than any minimum service temperature.[41] The DBTT of the other filler wires (309L, 309LSi, 316L) is estimated to be in the range of 0 - 25°F, based upon the fracture appearance transition temperature (FATT), described in detail in the Fractography section below.

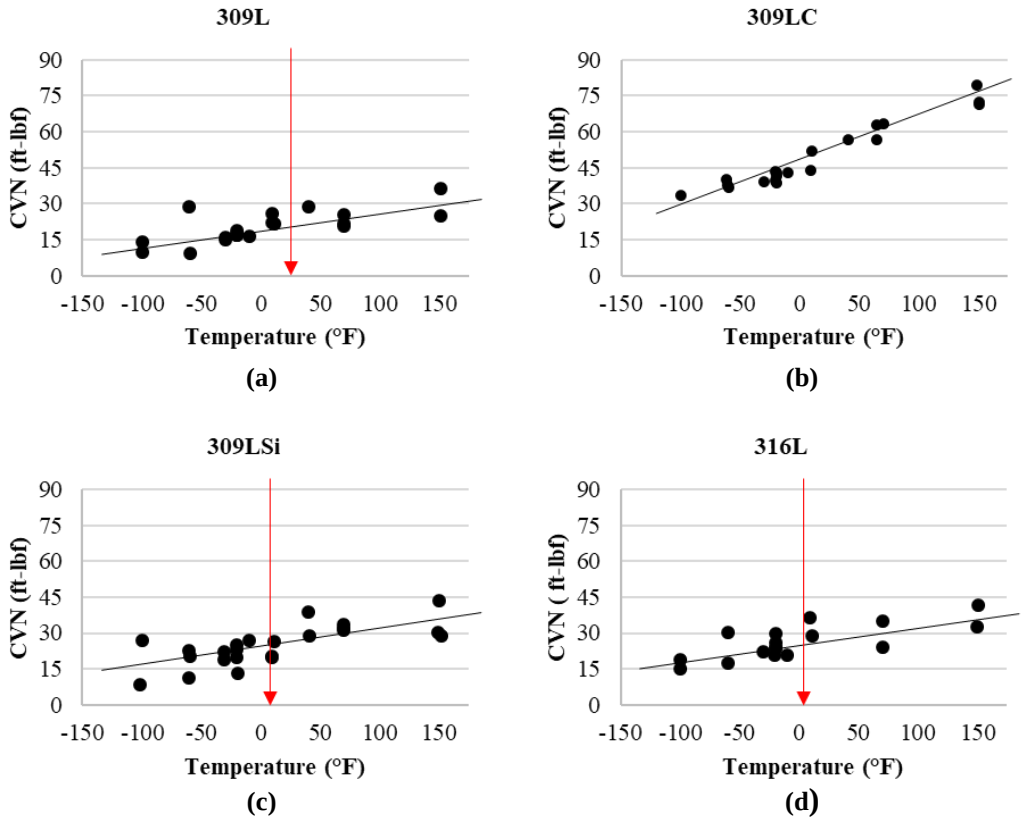

Figure 14. CVN data for the 1/2 in welded (Group 1) plates using a heat input of 75 kJ/in and a maximum interpass temperature of 450 °F for the entire range of service temperatures for welds made using 309L (a), 309LC (b), 309LSi (c), and 316L (d). The red arrow indicates the fracture appearance transition temperature (FATT), determined based on visual inspection, as described in more detail in the Fractography section below. (No FATT was observed for 309LC.)

Side Bend Testing

The four bend tests performed on each PQR plate were acceptable.[41] No cracks were observed in the weld when a full 180° bend was placed on the bend test sample. Figure 15 presents macroimages of a typical side bend test sample. This is consistent with available literature on bend testing of the legacy alloy, 3CR12, where no cracking within the coarse-grained HT-HAZ was observed when welding with austenitic filler wires that were employed in the present study.[8]

a) b)

Figure 15. a) Side view and b) top view of the side bend samples with the weld placed in the middle

Fractography

One method of characterizing CVN fracture surfaces is visual inspection and optical microscopy. Ductile fractures appear dull whereas brittle fractures (both intergranular and intragranular) will generally have a more granular appearance, which will more readily reflect light and appear shiny.[47,61] (During the course of the study, the nature of the fracture was also confirmed using SEM fractography.) Figure 16 shows the fracture surface appearance of welds made using all four filler wires at a heat input of 75 kJ/in and a maximum interpass temperature of 450 °F. Each row of figures corresponds to CVN tests performed at -100, -20 and 150 °F, from left to right. The first observation to be made is the ductile appearance of the fractures at all temperatures in the welds made using 309LC. Secondly, one can observe details about the appearance of the brittle fractures in the welds made using the other three (solid) filler wires. Note the large, bright regions, which are present, especially in Figures 16 (a, d, g, h) that correspond to the large prior δ-ferrite grains which extend parallel to the weld centerline in Figure 9 (a & b). The use of 309LC metal core filler wire results in the refinement of the δ-ferrite grains during solidification as well as the Widmanstätten structure adopted by the austenite within those grains during cooling (Figure 10). Thus, as alluded to in the Introduction, it is hypothesized that even though the ferrite content of the weld comprised of 309LC filler metal is higher than the others (Table 6), the distribution/morphology of that retained ferrite is not detrimental to the toughness. Indeed, the refined microstructure appears to be beneficial, in spite of the higher ferrite content.

Finally, since the CVN impact toughness of the welds do not exhibit the three-zone lower-shelf, upper-shelf, and transition region but instead exhibit linear transition curves, it was desirable to develop another means of establishing the DBTT. Therefore, the 50% ductile-50% brittle fracture appearance transition temperature (FATT) was determined by optical microscopy. The degree of ductile vs. brittle fracture surface appearance was quantified and the results were analyzed using linear regression to determine the best-fit temperature at which the 50:50 transition occurred, as indicated by arrows in Figure 17. These are the DBTT values, which are also indicated with arrows in Figure 14.

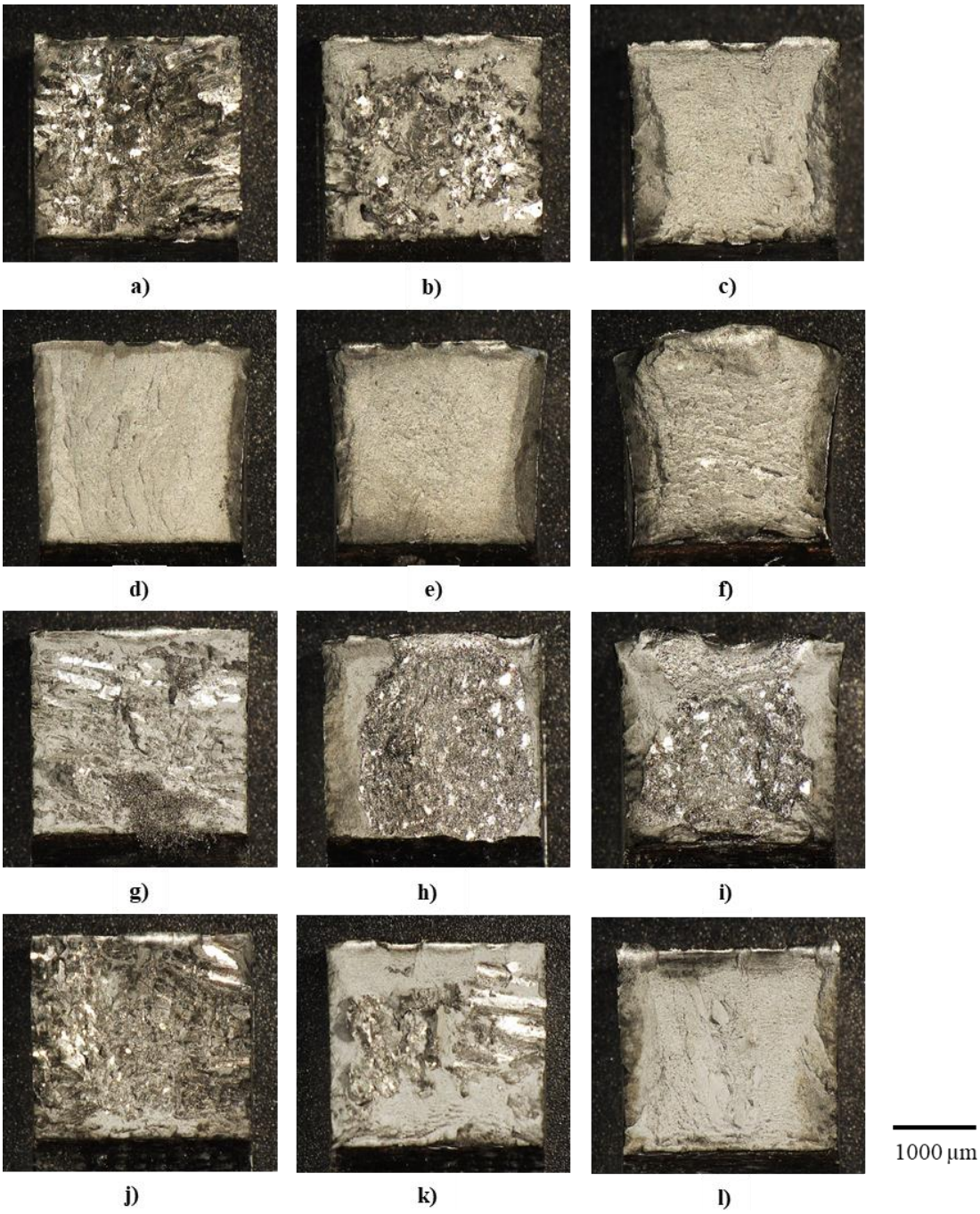

Figure 16. Optical micrographs of the CVN fracture surfaces taken at 20X magnification of the Group 1 samples welded using a heat input of 75 kJ/in and a maximum interpass temperature of 450 °F. Each row of figures corresponds to tests performed at -100 °F (a, d, g, j), -20 °F (b, e, h, k), and 150 °F (c, f, i, l) on welds made using 309L (a, b, c), 309LC (d, e, f), 309LSi (g, h, i), and 316L (j, k, l), respectively

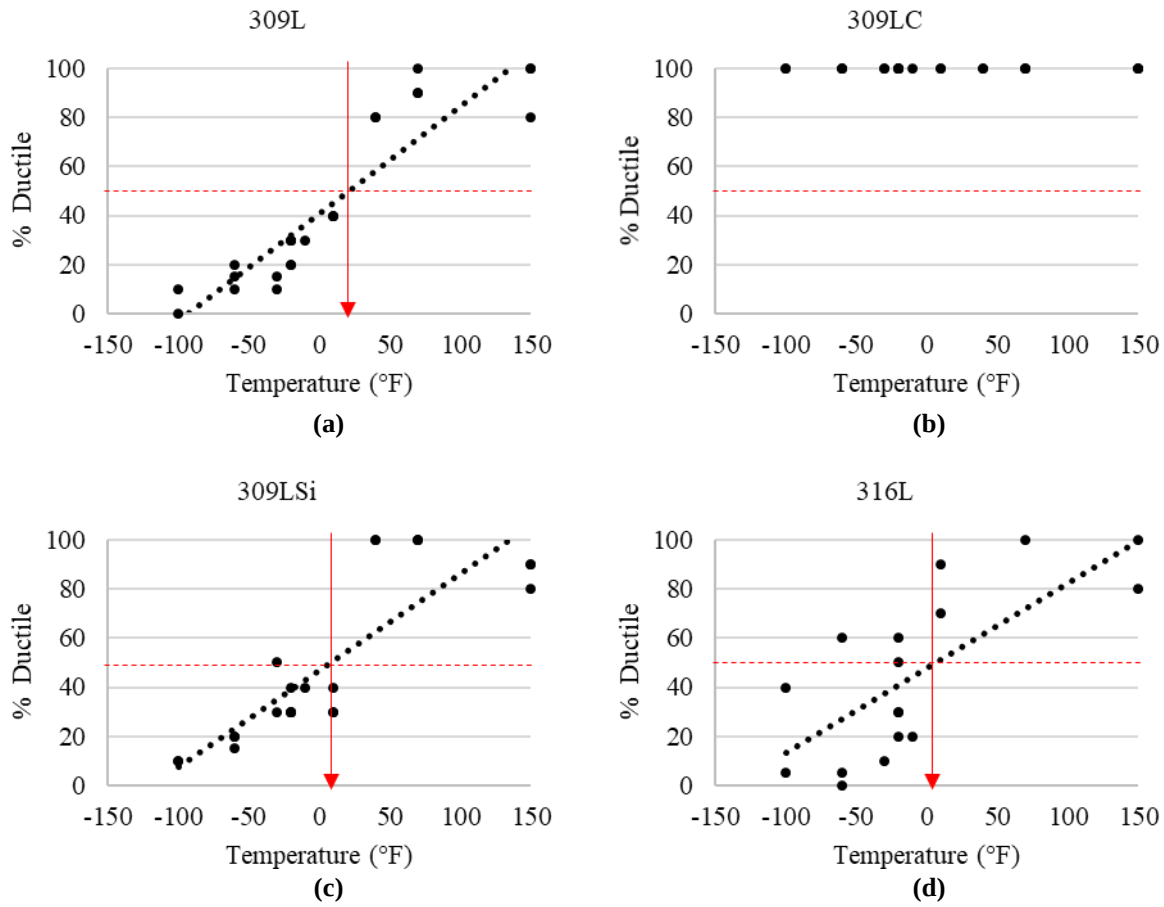

Figure 17. The FATT based on optical micrographs of the CVN fracture surfaces taken at 20X magnification of the Group 1 samples welded using a heat input of 75 kJ/in and a maximum interpass temperature of 450 °F for welds made using 309L (a), 309LC (b), 309LSi (c), and 316L (d).

CONCLUSIONS

- *The DBTT of the 50CR base plate was determined to be -40 °F, a marked improvement from that of conventional structural weathering steel 50W (-10 °F) and the legacy alloy 3CR12 (14 °F in LT orientation and 50 °F in the TL orientation).* Note that there is no statistically significant difference in the DBTT between the L and T orientations of 50CR base plate.

- *The following filler wires can be used as alternatives to 309L for the welding of 50CR: 309LC, 309LSi, and 316L.* Note that 309LC metal cored wire requires a higher feed rate (~50%), but other welding parameters (voltage, current, and travel speed) can remain the same.

- *The 309LC filler wire can be used to weld 1/2 in thick 50CR steel plates with heat inputs of up to 75 kJ/in and all interpass temperatures explored up to 450 °F.* Such welds exceed all mechanical property requirements.

- *Use of 309L filler wires for welding 1/2 in thick 50CR steel plates results in welds having borderline passing Charpy V-notch requirements at a heat input of 75 kJ/in at interpass temperatures ranging from 125 to 450 °F. The properties of welds produced with a heat input of 50 kJ/in exceeded all mechanical property requirements.*

- *Use of 309LSi and 316L filler wires for 1/2 in thick 50CR steel plates welded at a heat input of 75 kJ/in over the entire range of interpass temperatures explored (125 – 450 °F) produced welds which passed the Charpy V-notch requirements for non-fracture critical components, but did not pass the Charpy V-notch requirements for fracture critical components.*

- *The enhanced impact energy and low DBTT of welds in 1/2 in thick 50CR steel plates formed using 309LC filler wire appear to be due to the mitigation of large, aligned δ-ferrite grain formation during solidification and refinement of the austenite structure, which forms during cooling.* Otherwise, such large, aligned grains serve as preferred crack paths in welds.

- *Heat inputs of 90 kJ/in and interpass temperatures of up to 450 °F can be used for 309L, 309LC, 309LSi, and 316L filler wires for 1 in thick 50CR steel plate.* Thicker plates are more tolerant of high heat inputs because they represent a larger heat reservoir outside the fusion zone itself.

RECOMMENDATIONS

1. *VDOT Materials Division should allow for the use of 309L, 309LC, 309LSi, and 316L filler wires when welding 50CR steel.* This includes allowing the interpass temperature to be increased to 450°F with these alloys. For the 309L, 309LSi, and 316L filler wires, a maximum heat input of 50 kJ/in is recommended for ½ in thick plates. For the 309LC filler wire, the maximum heat input can be increased to 75 kJ/in for ½ in thick plates. For 1 in thick plates, VDOT Materials Division should allow an interpass temperature of 450°F, and a maximum heat input of 90 kJ/in is recommended for all filler wire alloys tested.

2. *VDOT Materials Division should allow for the use of higher feed rates with the 309LC filler wire, up to 50% higher, as compared to the other solid filler wires tested*.

3. *VTRC should work with VDOT Materials Division to evaluate the influence of plate thickness and details of 50CR steel weld microstructures, with the primary focus of this effort being on the HAZ.* Additional work should be performed by the VTRC to investigate the possibility that the failure mode observed during tensile testing in this project could indicate that 50CR steel fillet welds are susceptible to lamellar cracking.

4. *VTRC should work with VDOT Materials Division and a VDOT district to locate a practical location to use the 309LC filler wire in the butt joints of 50CR steel girder flanges for a proposed bridge.* During fabrication, as the weld quality is being evaluated and documented, additional samples should be produced and evaluated by VTRC for VDOT Materials Division.

IMPLEMENTATION AND BENEFITS

Implementation

- Implementation of Recommendations 1 and 2 will require VDOT Materials Division to update the current 50 CR special provision to incorporate these changes. Implementation of Recommendations 1 and 2 will occur within 1 year after the publication of this report.

- Implementation of Recommendation 3 will require VDOT's Materials Division (project Champion) and VTRC to first initiate a project to evaluate the influence of plate thickness on change in microstructure during welding. Then VDOT's Materials Division and VTRC should initiate a second project focused on investigating the possibility of lamellar tearing that was suggested by tensile test results. The VTRC will be tasked with determining if all work can be performed or if it requires a university contract to assist in meeting the objectives of this recommendation. Implementation of Recommendation 3 will occur within 4 years after the publication of this report.

- Implementation of Recommendation 4 will require VDOT's Materials Division (project Champion) and VTRC to initiate a project with a VDOT district to fabricate 50CR girders for a bridge. This will also require VTRC assist VDOT's Materials Division in revising a special provision that will incorporate the findings from this report. As part of this effort, VTRC will assist the district by providing guidance on the use of 50CR and other related structural components, as well as providing the cost difference due to the use of 50CR girders with 309LC welded butt-joints. Implementation of Recommendation 4 will occur within 4 years after the publication of this report.

Benefits

- The benefit of Recommendations 1 and 2 will improve competitiveness with prestressed CFRP and SS reinforced concrete beam products by increasing 50 CR girder fabrication productivity by allowing the use of addition filler wires and more favorable welding parameters. This also allows for the possibility of different filler wire companies to compete and eliminates the sole source requirement while satisfying the Buy America regulations.

- The benefit of Recommendations 3 and 4 allows VDOT to provide better guidance as specifications are developed by AWS and AASHTO for welding ASTM A709 Grade 50CR.

ACKNOWLEDGEMENTS

The authors are grateful to Justin Ocel of Federal Highway Administration Turner-Fairbank, Fred Fletcher of ArcelorMittal, Adam Steppe of High Steel Structures LLC, Bill Via of the Virginia Department of Transportation, Stephen Sharp, Jason Provines, Bill Ordel of the Virginia Transportation Research Council for their expertise and advisement of the project. The authors would also like to thank the Virginia Department of Transportation and the Virginia Transportation Research Council for their funding of this project.

REFERENCES

1. Fletcher, F.B. *Improved Corrosion-Resistant Steel for Highway Bridge Construction*. FHWA-HRT-11-062. Federal Highway Administration, Washington D.C., 2011.

2. Knutsen, R.D. *A Microstructural Examination of Duplex Ferrite-Martensite Corrosion Resisting Steels*. PhD dissertation. University of Cape Town, Cape Town, South Africa, 1989.

3. Balmforth, M.C., and Lippold, J.C. A Preliminary Ferritic-Martensitic Stainless Steel Constitution Diagram. *Welding Journal-Supplement*, Vol. 77, No. 1, 1998, pp. 1-7.

4. Balmforth, M.C., and Lippold, J.C. A New Ferritic-Martensitic Stainless Steel Constitution Diagram. *Welding Journal- Supplement*, Vol. 79, No. 3, pp. 339-345.

5. Ball, A., and Hoffman, J.P. Microstructure and Properties of a Steel Containing 12% Chromium. *Metals Technology*, Vol. 8, No. 1, 1981, pp. 329-338.

6. Matthews, L.M., and DeMarsh, E.A. *The Response of As-Rolled 3Cr12 Steel to Heat Treatment.* M213. Council for Mineral Technology, Randburg, South Africa, 1985.

7. Thomas, C.R. Structure and Properties of a Duplex Ferritic-Martensitic Stainless Steel. In *Duplex Stainless Steels*, R.A. Lula (Ed.). American Society of Metals, Metals Park, Ohio, 1983, pp. 649-664.

8. Grobler, C. *Weldability Studies on 12% and 14% Chromium Steels.* PhD dissertation. University of Pretoria, Pretoria, South Africa, 1987.

9. Jana, S. Effect of Heat Inputs on the HAZ Properties of Two Duplex Stainless Steels. *Journal of Materials Processing Technology*, Vol. 33, No. 3, 1992, pp. 247 – 261.

10. Hoffman, J.P. The Welding Metallurgy of a Titanium Stabilized 12 Percent Chromium Ferritic-Martensitic Steel. In *New Developments in Stainless Steel Technology*, R.A. Lula (Ed.). American Society of Metals, Metals Park, Ohio, 1985, pp. 305-318.

11. Taban, E., Deleu, E. Dhooge, A., and Kaluc, E. Laser Welding of Modified 12% Cr Stainless Steel: Strength, Fatigue, Toughness, Microstructure, and Corrosion Properties. *Materials and Design*, Vol. 30, No. 4, 2009, pp. 1193 – 2000.

12. Bennett, P. The Weldability of 12% Chromium Ferritic Corrosion-Resisting Steels. *Materials Australasia*, Vol. 23, No. 5, 1991, pp. 15-16.

13. Venkatesan, M.V., Murugan, N., Sam, S., and Albert, S.K. Effect of Heat Input on Macro, Micro, and Tensile Properties of Flux Cored Arc Welded Ferritic Stainless Steel Joints. *Transactions of the Indian Institute of Metals*, Vol. 67, No. 3, 2014, pp. 375-383.

14. Okasha, N.M., Frangopol, D.M., Fletcher, F., and Wilson, A.D. Life-Cycle Cost Analyses of a New Steel for Bridges. *Journal of Bridge Engineering,* Vol. 17, No. 1, 2012, pp. 168 – 172.

15. Soliman, M. and Frangopol, D.M. Life-Cycle Cost Evaluation of Conventional and Corrosion-Resistant Steel for Bridges. *Journal of Bridge Engineering*, Vol. 20, No. 1, 2015, pp. 06014005.

16. ArcelorMittal. https://usa.arcelormittal.com/.../steel-products/plate-products/Duracorr-lifecycle.pdf, Accessed July 7, 2016.

17. Toit, M. du., Naude, J. The influence of stabilization with Titanium on the Heat-Affected Zone Sensitization of 11 to 12 % chromium ferritic stainless steels under low heat input welding conditions. *Welding in the World*, Vol. 55, No 03/04, 2011, pp. 38-47

18. van Warmelo, M., Nolan, D. and Norrish, J. Mitigation of Sensitisation Effects in Unstabilised 12%Cr Ferritic Stainless Steel Welds. *Materials Science and Engineering A*, Vol. 464A, No. 1-2, 2007, pp. 157–169.

19. Amuda, M.O.H. and Mridha, S. An Overview of Sensitization Dynamics in Ferritic Stainless Steel Welds. *International Journal of Corrosion,* 2011.

20. Lakshminarayanan, A.K. and Balasubramanian, V. Assessment of Sensitization Resistance of AISI 409M Grade Ferritic Stainless Steel Joints Using Modified Strauss Test. *Materials and Design,* Vol. 39, 2012, pp. 175–185.
21. Seradj, H. Weldability of ASTM A1010 Steel. *Proceedings of 8th International Conference on Short and Medium Span Bridge*, Niagara Falls, Ontario, Canada, 2010.

22. Provines, J.T., Sharp, S.R., Ozbulut, O., and Daghash, S. *Maintenance-Free Corrosion-Resistant Steel Plate for Bridges*. FHWA/VTRC 19-R21. Virginia Transportation Research Council, Charlottesville, VA, 2019.

23. Seradj, H. Oregon's Experience with ASTM A1010. In *TRB 94th Annual Meeting Compendium of Papers,* Transportation Research Board of the National Academies, Washington D.C., 2015.

24. ArcelorMittal USA. https://usa.arcelormittal.com/~/media/Files/A/Arcelormittal-USA-V2/what-we-do/steel-products/plate-products/Duracorr-welding.pdf, Accessed December 10, 2019.

25. Easterling, K. E. *Introduction to the Physical Metallurgy of Welding.* Butterworth-Heinemann Ltd., Jordan Hill, Oxford, 1992.

26. DuPont, J.N. Dilution in Fusion Welding. In *ASM Handbook: Welding Fundamentals and Processes*, Vol. 6A, Materials Park, OH, 2011, pp. 115-121.

27. David, S.A., and Vitek, J.M. Embrittlement of Austenitic Stainless Steel. CP 95330. Oak Ridge National Lab, U.S. Department of Energy, 1997. https://www.osti.gov/biblio/563198-embrittlement-austenitic-stainless-steel-welds. Accessed July 22, 2019.

28. The Lincoln Electric Company. https://www.lincolnelectric.com/assets/US/EN/literature/c64000.pdf, Accessed July 8, 2019.

29. Mateša, B., Samardžić, I., and Dunđer, M. The Influence of the Heat Treatment on Delta Ferrite Transformation in Austenitic Stainless Steel Welds. *Metalurgija*, Vol. 51, No. 2, 2012, pp. 229-232.

30. Lundin, C.D., Ruprecht, W., and Zhou, G. *Ferrite Measurement in Austenitic and Duplex Stainless Steel Castings.* 13734-1. Steel Founder's Society of America/Cast Metals Coalition/Department of Energy, 1999. https://www.osti.gov/biblio/14577/. Accessed July 11, 2019.

31. Schaeffler, A.L. Constitution Diagram for Stainless Steel Weld Metal. *Metal Progress*, Vol. 56, No. 2, 1949, pp. 680-680B.

32. DeLong, W.T., Ostrom, G.A., and Szumachowski, E.R. Measurement and Calculation of Ferrite in Stainless Steel Weld Metal. *Welding Journal- Supplement*, Vol. 35, No. 2, 1956, pp. 521-528.

33. Niagaj, J., and Mazur, L. Review of Methods for Measurement of Ferrite Content in High Alloyed Steels and Their Welded Joints. *Welding International*, Vol. 28, No. 3, 2014, pp. 345-353.

34. TWI. https://www.twi-global.com/technical-knowledge/job-knowledge/welding-of-austenitic-stainless-steel-103, Accessed November 20, 2019.

35. Shankar, V., Gill, T. P. S., Mannan, S. L., & Sundaresan, S. (2003). Solidification cracking in austenitic stainless steel welds. *Sadhana*, *28*(3-4), 359-382.

36. Wang, P., Lu, S. P., Xiao, N. M., Li, D. Z., & Li, Y. Y. (2010). Effect of delta ferrite on impact properties of low carbon 13Cr–4Ni martensitic stainless steel. *Materials Science and Engineering: A*, *527*(13-14), 3210-3216.

37. Kotecki, D. J. Ferrite Control in Duplex Stainless Steel Weld Metal. *Welding Research Supplement*, Vol. 65, 1986, pp. 1273-1278.

38. Koseki T, Flemings M C 1996 Solidification of undercooled Fe–Cr–Ni alloys part II – microstructural evolution. Metall. Mater. Trans. A27: 3226–3240

39. Karlsson, L., Arcini, H., Bergquist, E.L., Weidow, J., Börjesson, J. Effects of Alloying Concepts on Ferrite Morphology and Toughness of Lean Duplex Stainless Steel Weld Metals. *Welding in the World*, Vol. 54, 2010, pp. 350-359.

40. Federal Highway Administration. *Bridge Welding Reference Manual.* FHWA-HIF-19-088. Federal Highway Administration, Washington D.C., 2019.

41. American Welding Society. *AASHTO/AWS D1.5M/D1.5:2015 Bridge Welding Code - Stainless Steel*, New York, NY, 2015.

42. ASTM International. *ASTM E1019-18 Standard Practice for Describing and Specifying Inductively Coupled Plasma Atomic Emission Spectrometers.* West Conshohocken, PA, 2018. www.astm.org

43. ASTM International. *ASTM E1479-16 Standard Test Methods for Determination of Carbon, Sulfur, Nitrogen, and Oxygen in Steel, Iron, Nickel, and Cobalt Alloys by Various Combustion and Inert Gas Fusion Techniques.* West Conshohocken, PA, 2016, www.astm.org.

44. Leng, Y. *Materials Characterization: Introduction to Microscopic and Spectroscopic Methods*. (John Wiley and Sons (Asia) Private Limited ed.) John Wiley and Sons, Singapore, 2008.

45. ASTM International. *ASTM E407-07(2015)e1 Standard Practice for Microetching Metals and Alloys.* West Conshohocken, PA, 2015, www.astm.org.

46. ASTM International. *ASTM A370-16 Standard Test Methods and Definitions for Mechanical Testing of Steel Products*. West Conshohocken, PA, 2016, www.astm.org.

47. ASTM International. *ASTM E23-16b Standard Test Methods for Notched Bar Impact Testing of Metallic Materials*. West Conshohocken, PA, 2017, www.astm.org.

48. ASTM International. *ASTM A709/A709M-17 Standard Specification for Structural Steel for Bridges*. West Conshohocken, PA, 2017, www.astm.org

49. Federal Highway Administration. https://www.fhwa.dot.gov/construction/contracts/buyam_qa.cfm. Accessed November 6, 2019.

50. Prajapati, P., and Badheka, V.J. Investigation on Various Welding Consumables on Properties of Carbon Steel Material in Gas Metal Arc Welding Under Constant Voltage Mode. *Sādhanā*, Vol. 42, No. 10, 2017, pp. 1751-1761.

51. ESAB. http://www.esabna.com/us/en/education/blog/advantages-and-disadvantages-of-metal-cored-wires.cfm. Accessed July 26, 2018.

52. Polymet. https://polymet.wordpress.com/2012/03/19/the-benefits-of-using-metal-cored-wire/. Accessed May 15, 2018.

53. Lyttle, K.A. Metal Cored Wires: Where Do They Fit in Your Future? *Welding Journal*, Vol. 75, 1996, pp. 35-38.

54. Select Arc Inc. http://www.select-arc.com/products/pdf/master_select-arc_catalog_9.15-new.pdf. Accessed October 28, 2018.

55. ASTM International. *ASTM A751-14a Standard Test Methods, Practices, and Terminology for Chemical Analysis of Steel Products*. West Conshohocken, PA, 2014, www.astm.org.

56. Meyer, A.M. *Interstitial Diffusion from the Weld Metal into the High Temperature Heat Affected Zone in 11-12% Chromium Steel Welded Joints*. Master's Thesis. University of Pretoria, South Africa, 2000.

57. Lundin, C. D., Delong, W. T., Spond, D. F. Ferrite-Fissuring Relationship in Austenitic Stainless Steel Weld Metals. *Welding Journal- Supplement*, Vol. 54, No. 2, 1975, pp. 241-246.

58. Akinlabi, E. T., Akinlabi, S. A. Characterising the Effects of Heat Treatment on 3CR12 and AISI 316 Stainless Steel. *International Journal of Mechanical, Aerospace, Industrial, Mechatronic, and Manufacturing Engineering*, Vol. 8, No. 2, 2014, pp. 256 – 261.

59. Lippold, J.C. *Welding Metallurgy and Weldability (*Wiley First ed.). John Wiley and Sons Inc., Hoboken, New Jersey, 2015, pp. 190-201.

60. *Steel Bridge Design Handbook*. FHWA-HIF-16-002. Federal Highway Administration, Washington D.C., 2015.

61. Blum, F., Comins, N.R., and Weiss, B.Z. The Influence of Microstructural Parameters on the Yield Stress and Impact energy of 3CR12 Steel. *Journal of the South African Institute of Mining and Metallurgy,* Vol. 92, 1992, pp. 185-193.

62. Arcelor Mittal https://usa.arcelormittal.com/.../steel-products/plate-products/Duracorr-Bridge.pdf. Accessed December 14, 2016.

63. Hertzberg, R.W., R.P. Vinvi, and J.L. Hertzberg. *Deformation and Fracture Mechanics of Engineering Materials (*Wiley India ed.), Daryaganj, New Delhi, 2014, pp. 307-314.

64. Sieurin, H. *Impact energy Properties of Duplex Stainless Steels*. PhD dissertation. Royal Institute of Technology, Stockholm, Sweden, 2006.

65. Dieter, G.E. *Mechanical Metallurgy* (McGraw Hill Education (India) Private Limited ed.). McGraw Hill, Inc., Chennai, India, 2013

APPENDIX A: CUT DIAGRAMS

The Charpy V-Notch (CVN) sample block contained 24 samples for the Group 1 plates welded using a heat input of 75 kJ/in and a maximum interpass temperature of 450 °F. Five CVN samples were machined for the plates welded using all fillers. An additional set of five CVN samples were tested for the Group 1 plates welded using 309L and 309LC. Each block of reduced area tension samples contained five samples. An additional set of five reduced area tension bars were tested for the Group 1 plates welded using 309L and 309LC. The CVN block contained five samples for the Group 2 plates. The reduced area tension block contained three samples. *Note:* All of the dimensions are in inches.

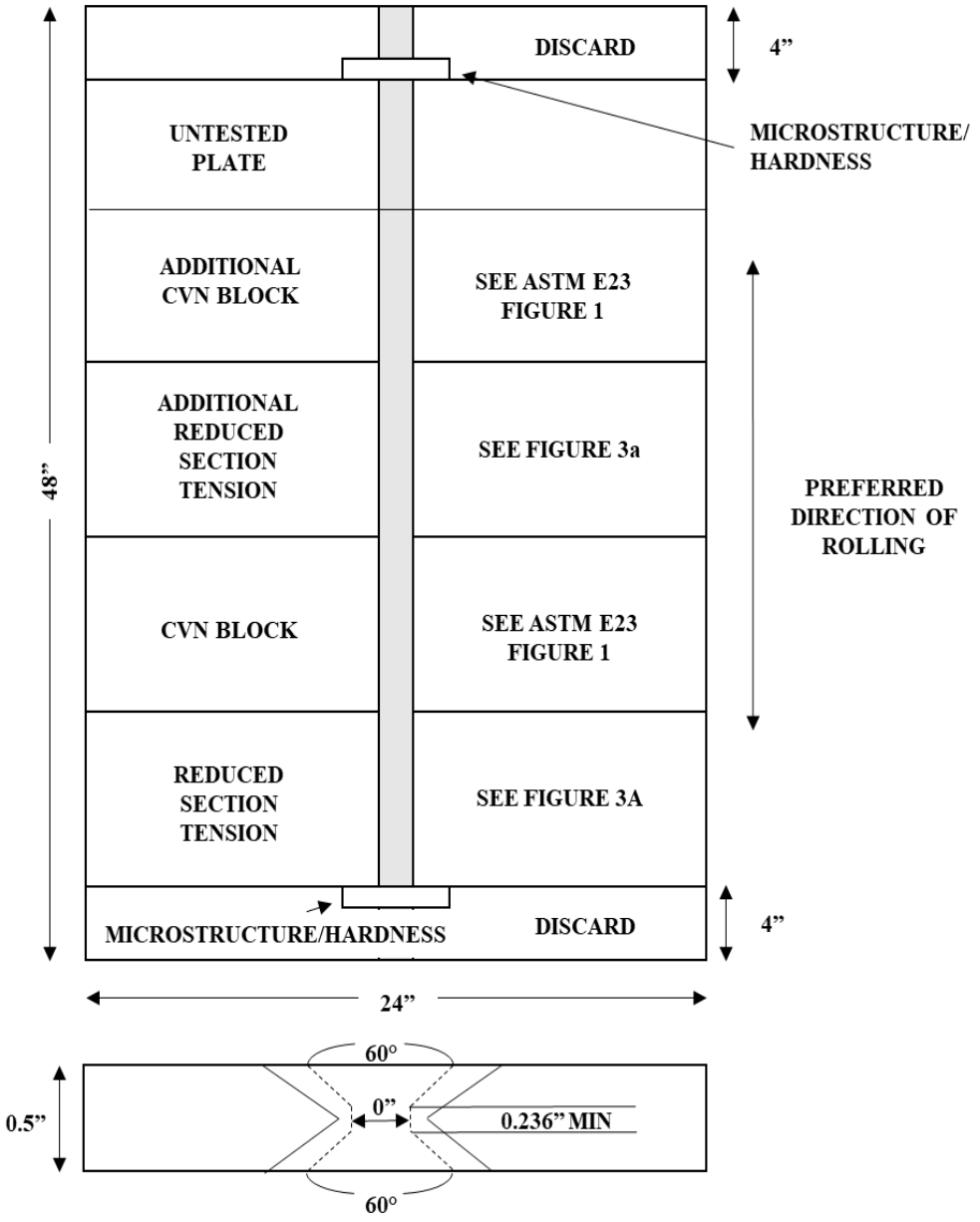

Figure A.1. Group 1 sample configuration map with only welded plate samples shown

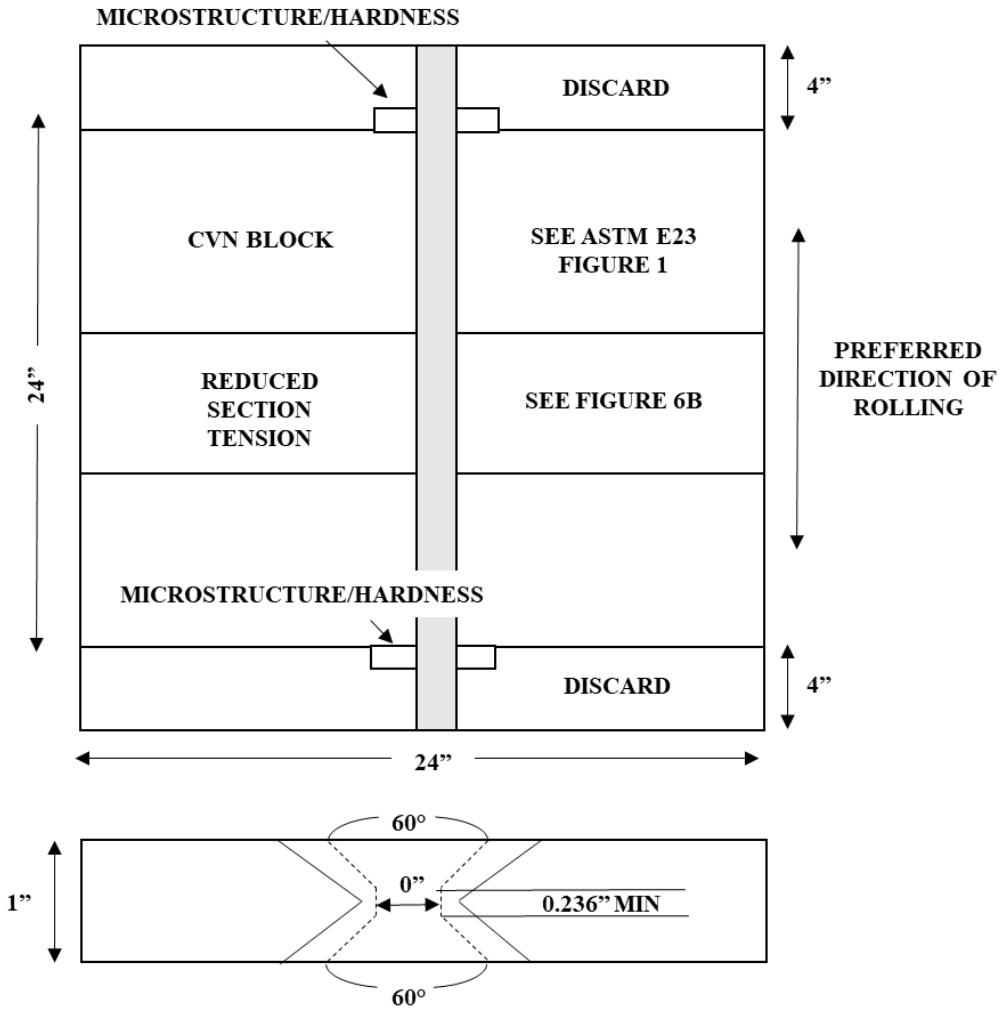

Figure A.2. Group 2 sample configuration map

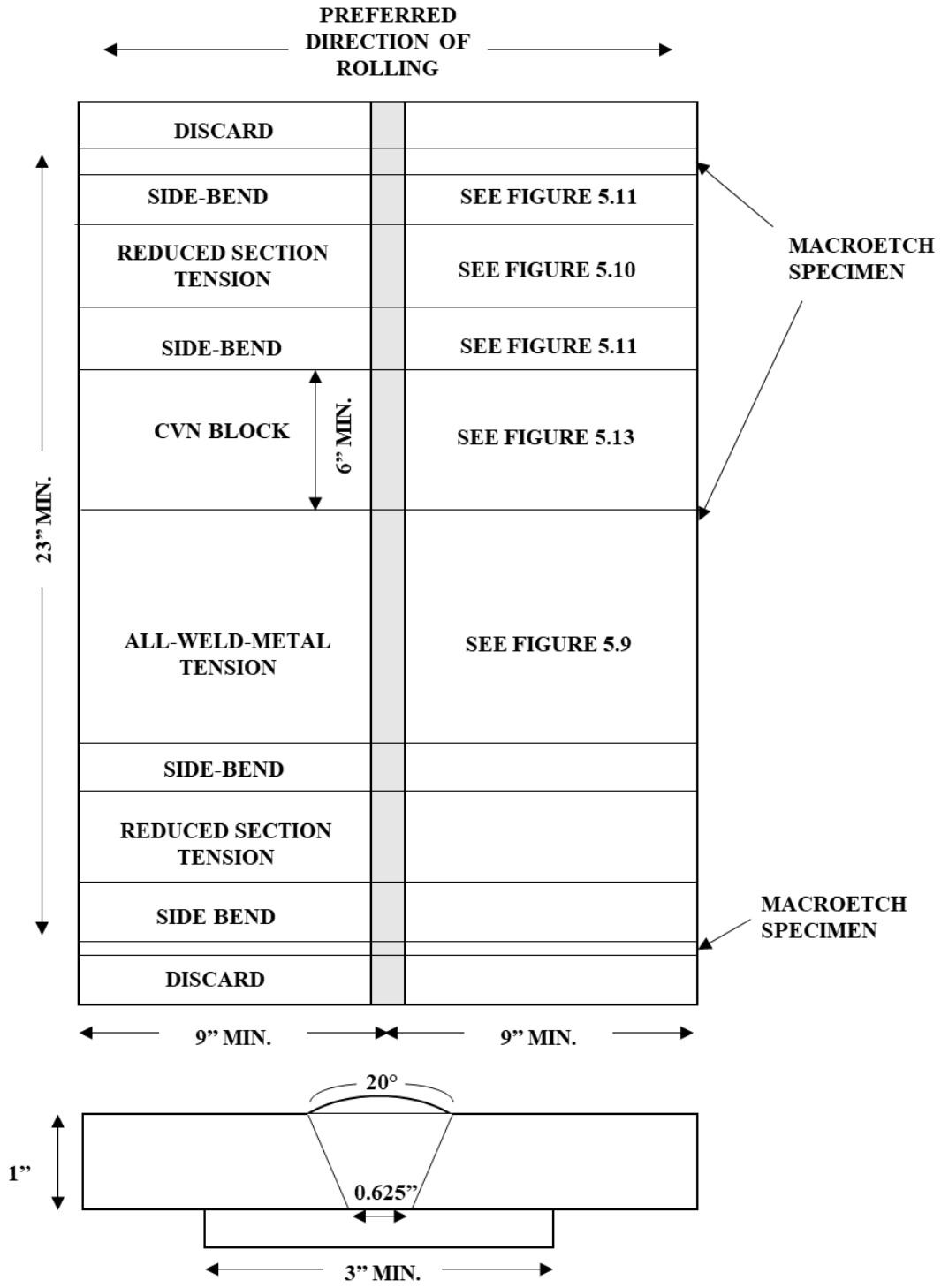

Figure A.3. Group 3 (PQR) plate sample configuration in accordance to AWS D1.5 PQR Plate A

APPENDIX B: MECHANICAL DATA FOR DEFECTIVE GROUP 1 PLATE

During tensile testing, it was discovered that the samples from the plate welded using 309LC, a heat input of 75 kJ/in, and a maximum interpass temperature of 300 °F contained a lack of fusion defect, a gap of roughly 0.0787 in (2 mm) in size, which was visible during radiography. Communications with the girder fabricator indicated that the weld gap arose from improper weld groove alignment and not from difficulty welding with the metal cored wire. Nevertheless, mechanical testing of the plate was performed as if there was no mechanical flaw.

The samples from the plate with a 2 mm gap (309LC, 75 kJ/in, 300 °F) resulted in an average yield strength of 55.2 ksi with a standard deviation of 0.76 ksi. This means that the plate would have met the ASTM A709 requirements.[40] The one-sided t-test also showed with 99% confidence that a sample chosen at random from the defective plate would have been able to meet the minimum requirements. Because the yield strength is the amount of stress a sample can undergo before yielding and beginning to plastically deform, a gap of this size is shown to be tolerable. This is helpful information to guide non-destructive evaluation requirements.

The samples from the plate with the incomplete weld (309LC, 75 kJ/in, 300 °F) yielded an average tensile strength of 69.9 ksi with a standard deviation of 3.42 ksi. This means that the plate would have met the ASTM A709 requirements, due to rounding. However, it fails the one-sided T-test for 90% confidence. This is due to the existence of the 2 mm gap, which acted like a pre-existing crack, resulting in a lower tensile strength.

The CVN impact energies for the plate with the incomplete weld is given below in Table B.1. Although there was a 0.0787 in (2mm) gap, the machining of the V-notch eliminated a majority of the welding defect. However, some of the welding gap still remained, which caused a decrease in the impact energy because the sample was already pre-cracked. The remaining weld gap simply continued to split, eliminating the need for a crack path to develop.

Table B.1. CVN impact energy for the defective plate

Filler Wire	Heat Input (kJ/in)	Maximum Interpass Temp. (°F)	CVN All 5 Samples (ft·lbf)	AWS D1.5 CVN (ft·lbf)
309LC*	75	300	22	22
309LC Retest*	75	300	24	24

Overall, the mechanical testing of the defective plate would have passed according to the AWS D1.5 requirements. This is further indication of the advantages that come with using 309LC filler wire. These results could also indicate that the non-destructive evaluation requirements for the welding of 50CR using 309LC filler wire could be relaxed. However, further testing of welded plate with planned defects must be performed before a firm conclusion on this point could be made.

APPENDIX C: FERRITE CONTENTS IN FUSION ZONES

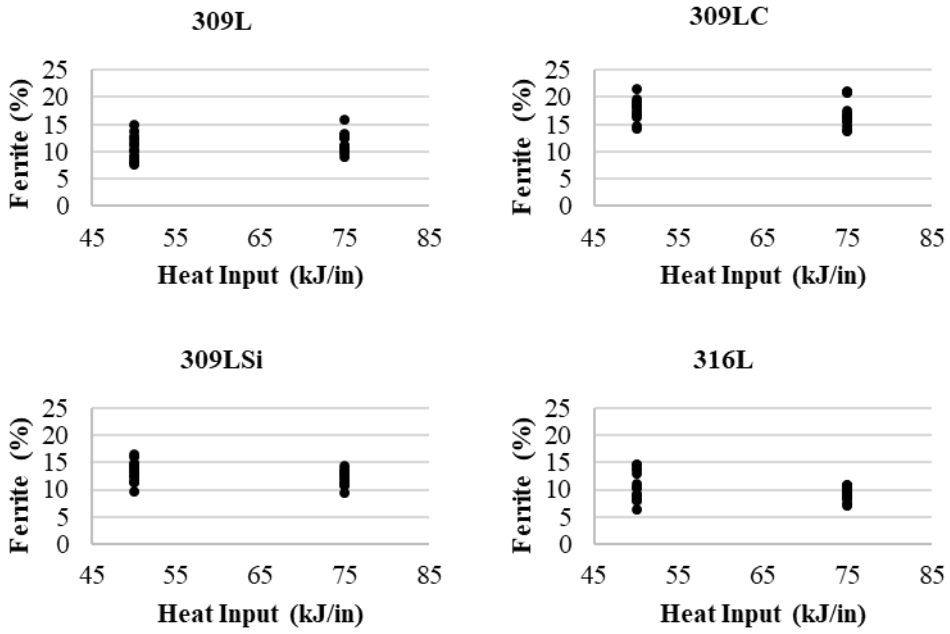

Figure C.1. Plots of the ferrite content as a function of heat input while keeping the maximum interpass temperature constant at 300 °F on Group 1 plates

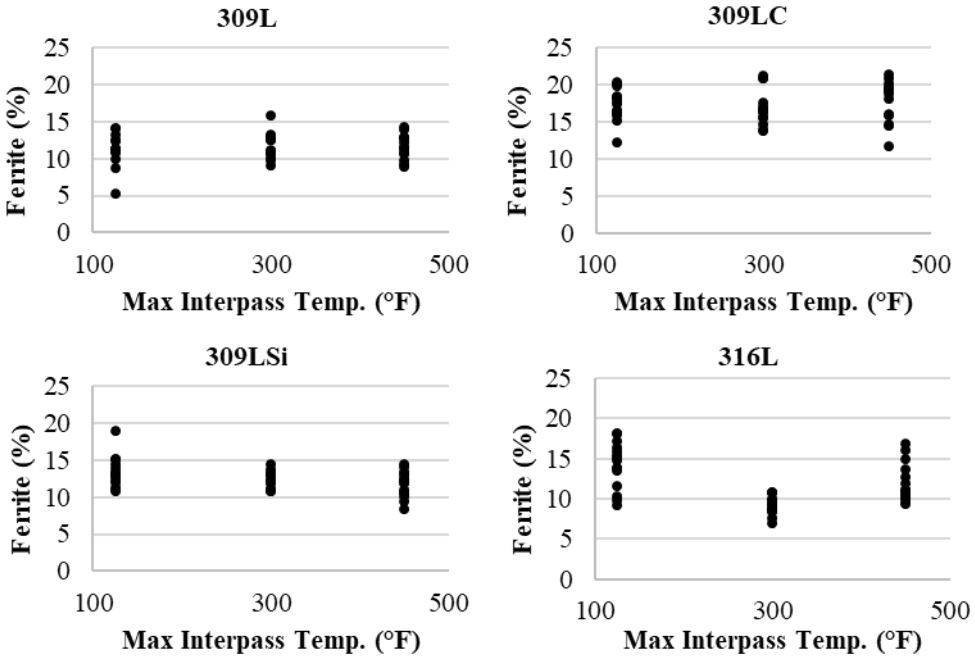

Figure C.2. Plots of the ferrite content as a function of maximum interpass temperature while keeping the heat input is held constant at 75 kJ/in on Group 1 plates

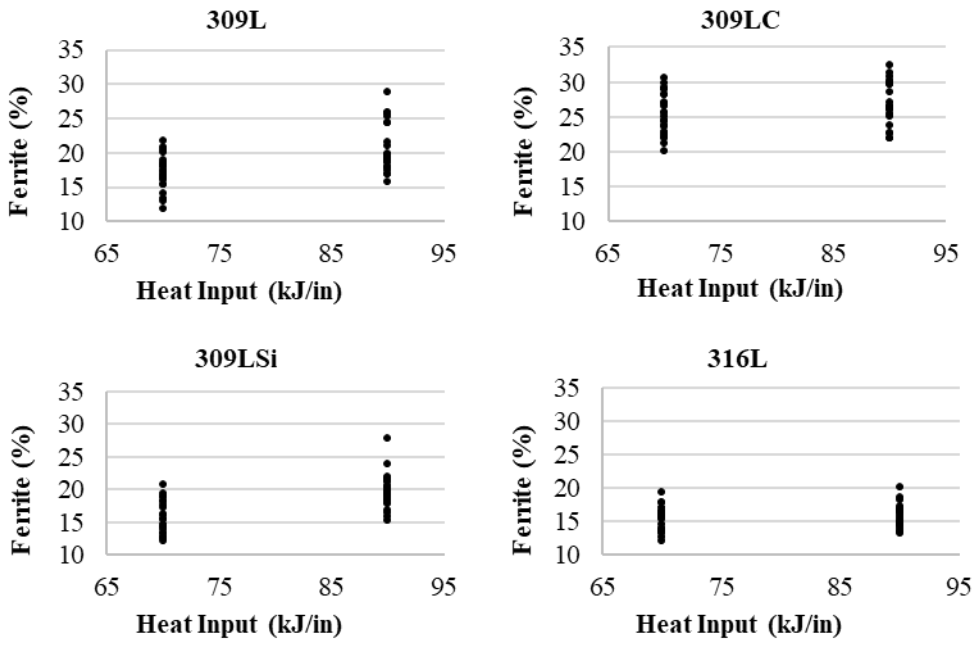

Figure C.3. Plots of the ferrite content as a function of heat input while the maximum interpass temperature constant at 300 °F on Group 2 plate

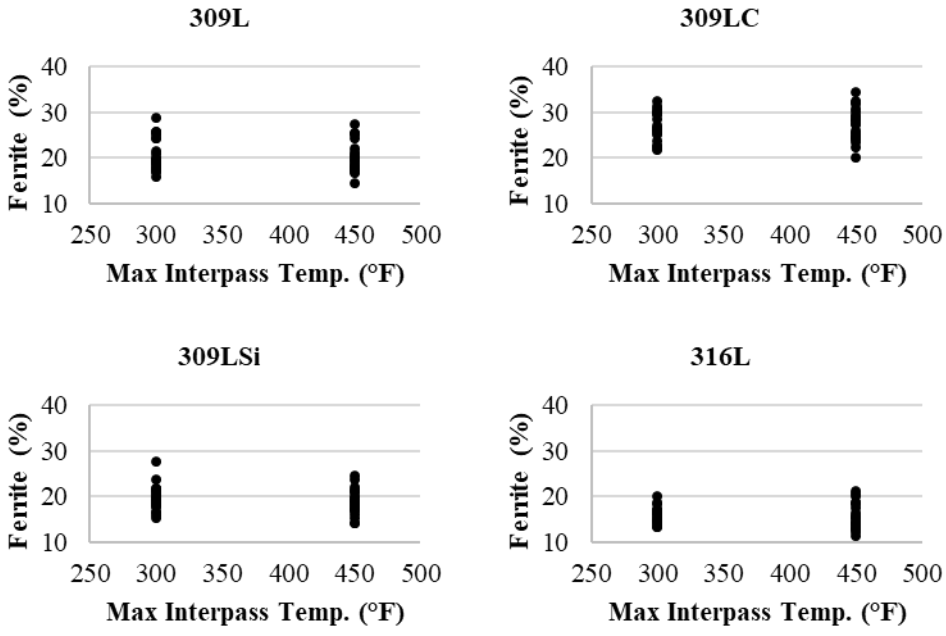

Figure C.4. Plots of the ferrite content as a function of maximum interpass temperature while keeping the heat input is held constant at 90 kJ/in on Group 2 plates

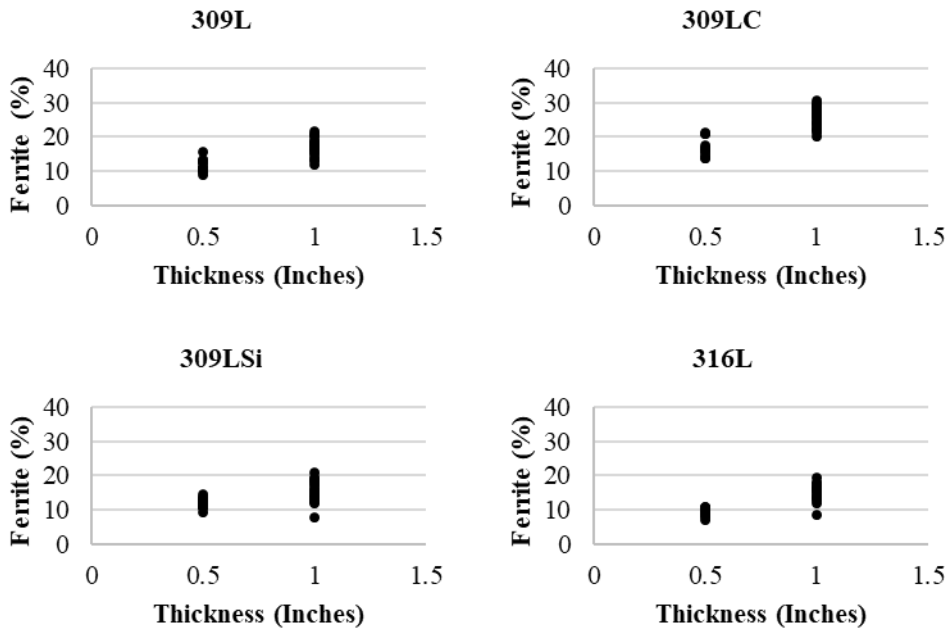

Figure C.5. Plot of the ferrite content as a function of plate thickness while keeping the heat input is held constant at 70-75 kJ/in and the maximum interpass temperature is held constant at 300 °F

APPENDIX D: TENSILE STRENGTH PROPERTIES OF WELDED PLATES

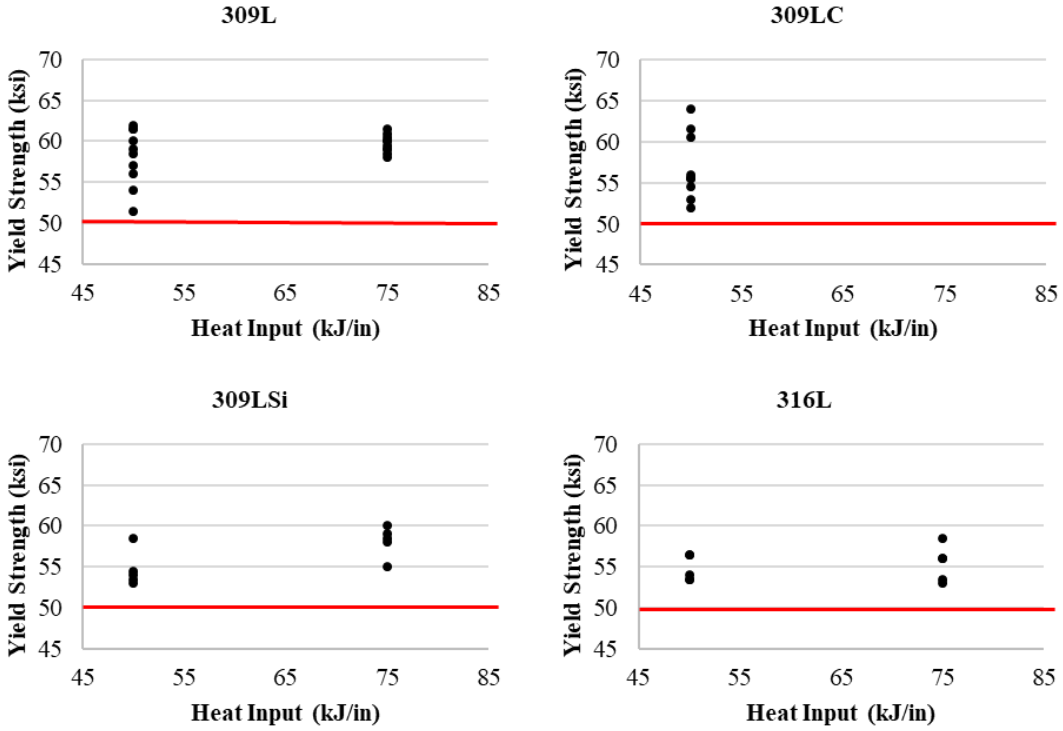

Figure D.1. Yield strength as a function of heat input while keeping the maximum interpass temperature constant at 300 °F of all Group 1 plates. ASTM A709 minimum requirement in red

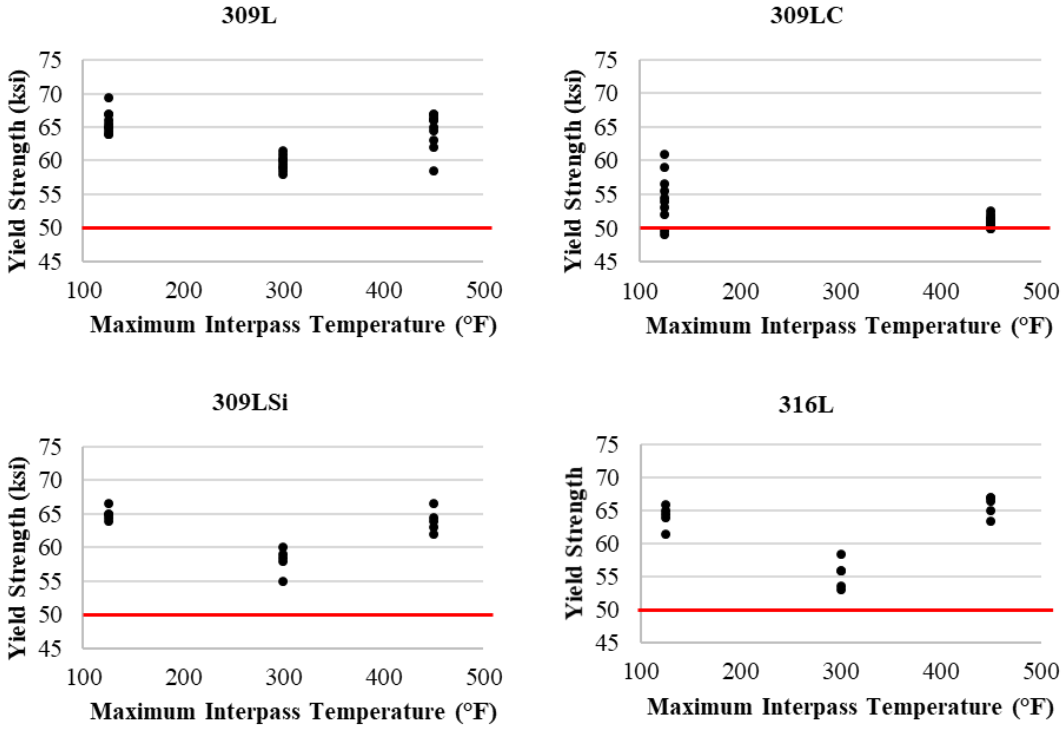

Figure D.2. Yield strength as a function of maximum interpass temperature while keeping the heat input constant at 75 kJ/in of all Group 1 plates. ASTM A709 minimum requirement in red.

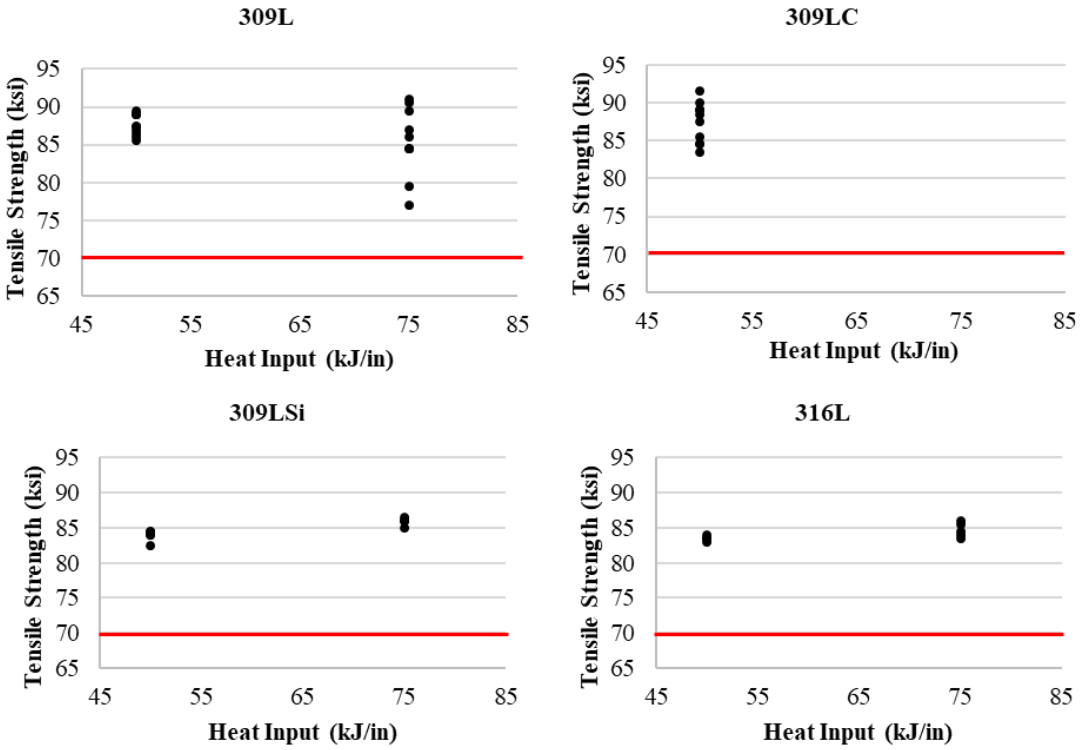

Figure D.3. Tensile strength as a function of heat input while keeping the maximum interpass temperature constant at 300 °F of all Group 1 plates. ASTM A709 minimum requirement in red.

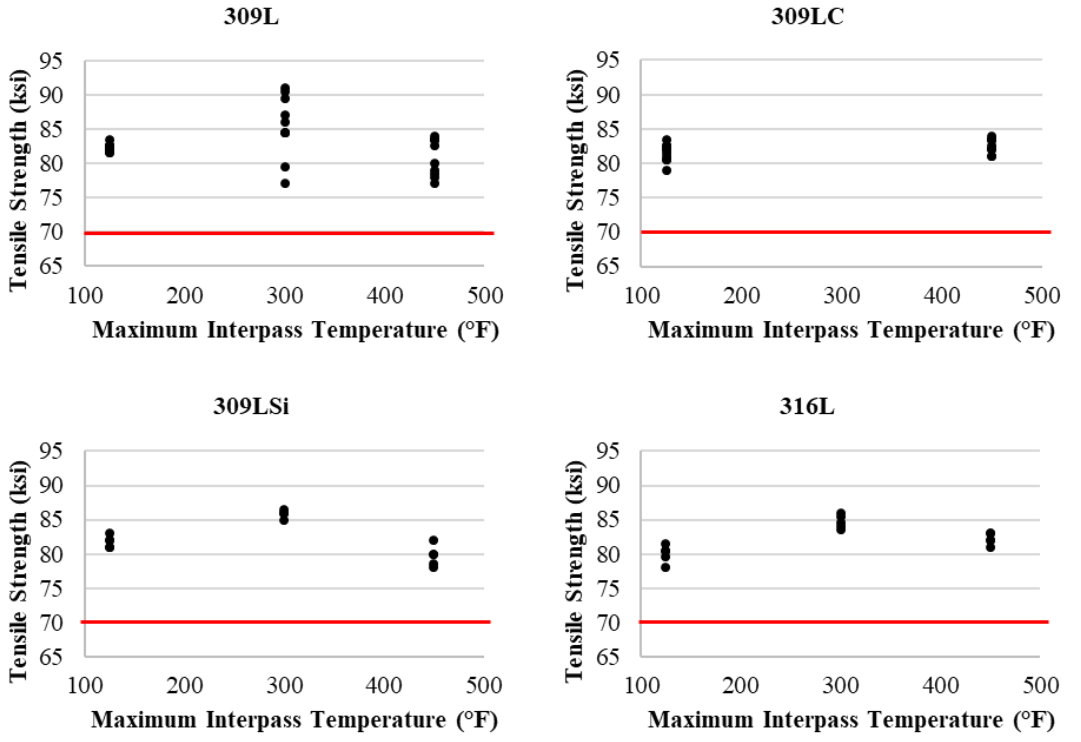

Figure D.4. Tensile strength as a function of maximum interpass temperature, while keeping the heat input constant at 75 kJ/in of all Group 1 plates. ASTM A709 minimum requirement in red.

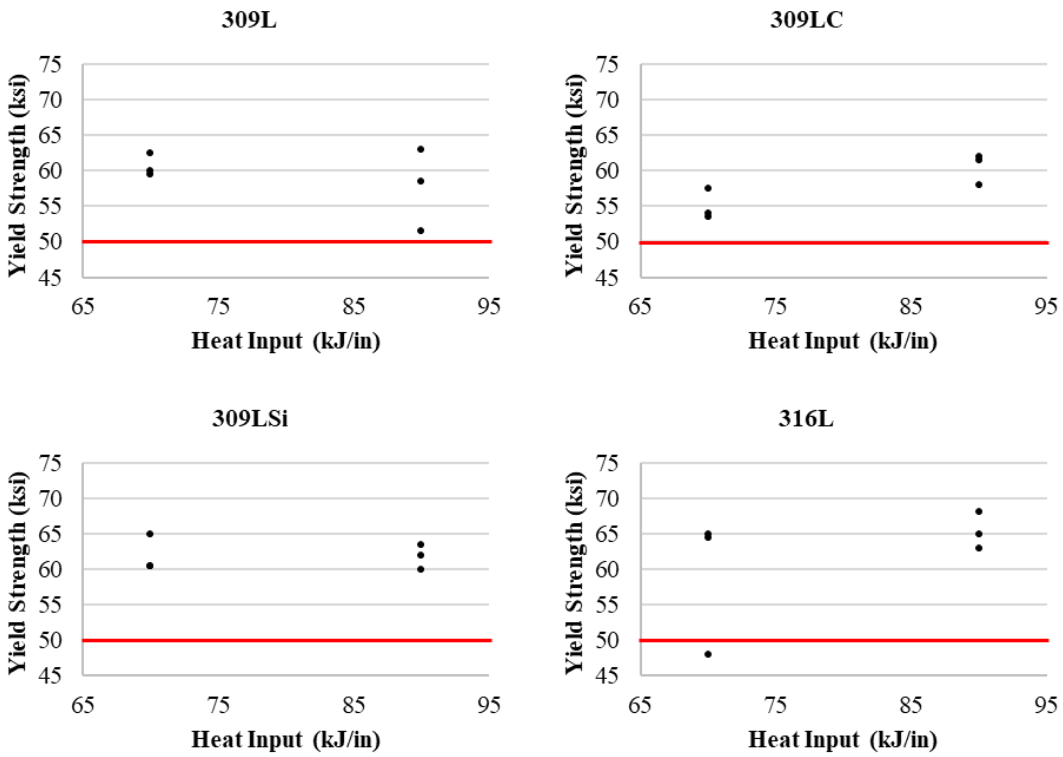

Figure D.5. Yield strength as a function of heat input while keeping the maximum interpass temperature constant at 300 °F of all Group 2 plates. ASTM A709 minimum requirement in red

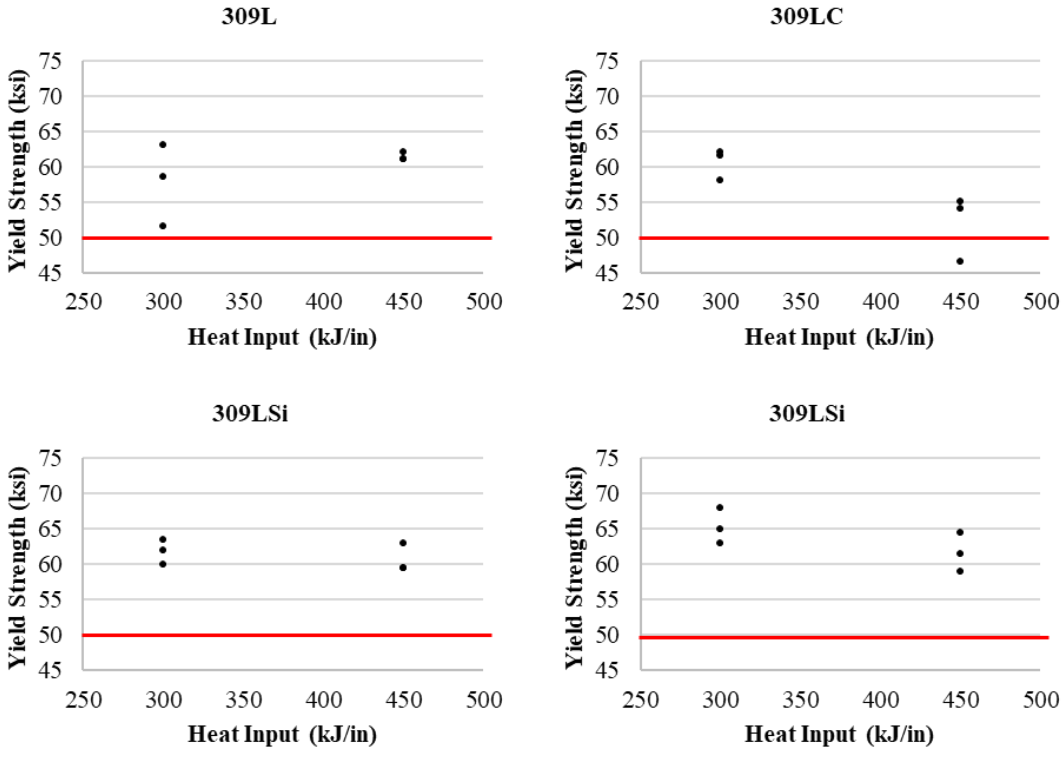

Figure D.6. Yield strength as a function of maximum interpass temperature while keeping the heat input constant at 90 kJ/in of all Group 2 plates. ASTM A709 minimum requirement in red

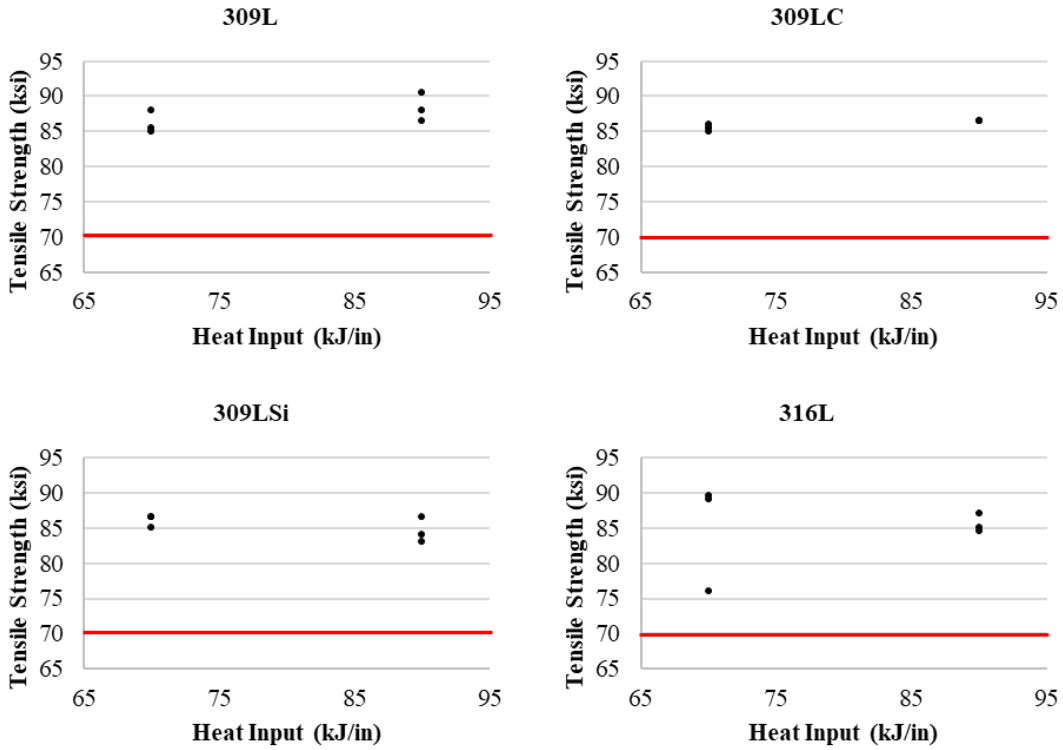

Figure D.7. Tensile strength as a function of heat input while keeping the maximum interpass temperature constant at 300 °F of all Group 2 plates. ASTM A709 minimum requirement in red

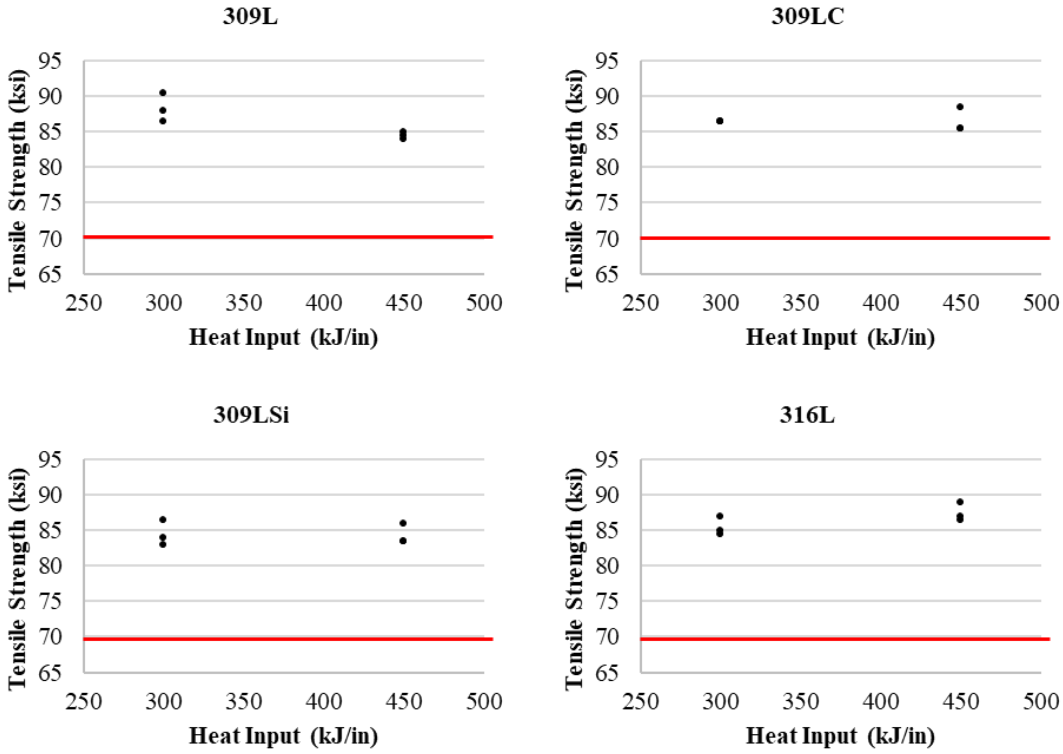

Figure D.8. Tensile strength as a function of maximum interpass temperature while keeping the heat input constant at 90 kJ/in of all Group 2 plates. ASTM A709 minimum requirement in red

APPENDIX E: CHARPY IMPACT TEST DATA

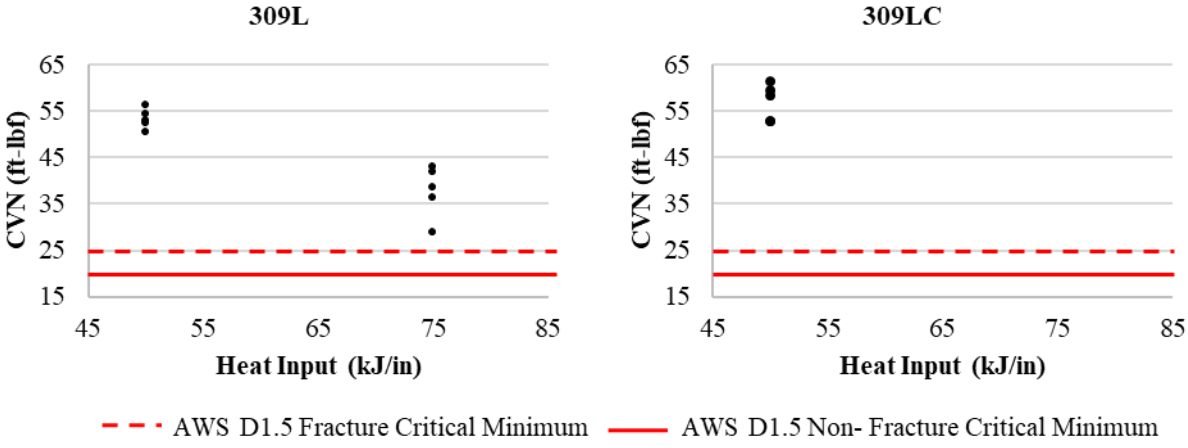

Figure D.9. CVN impact energy as a function of the heat input while keeping the maximum interpass temperature constant at 300 °F of all Group 1 plates

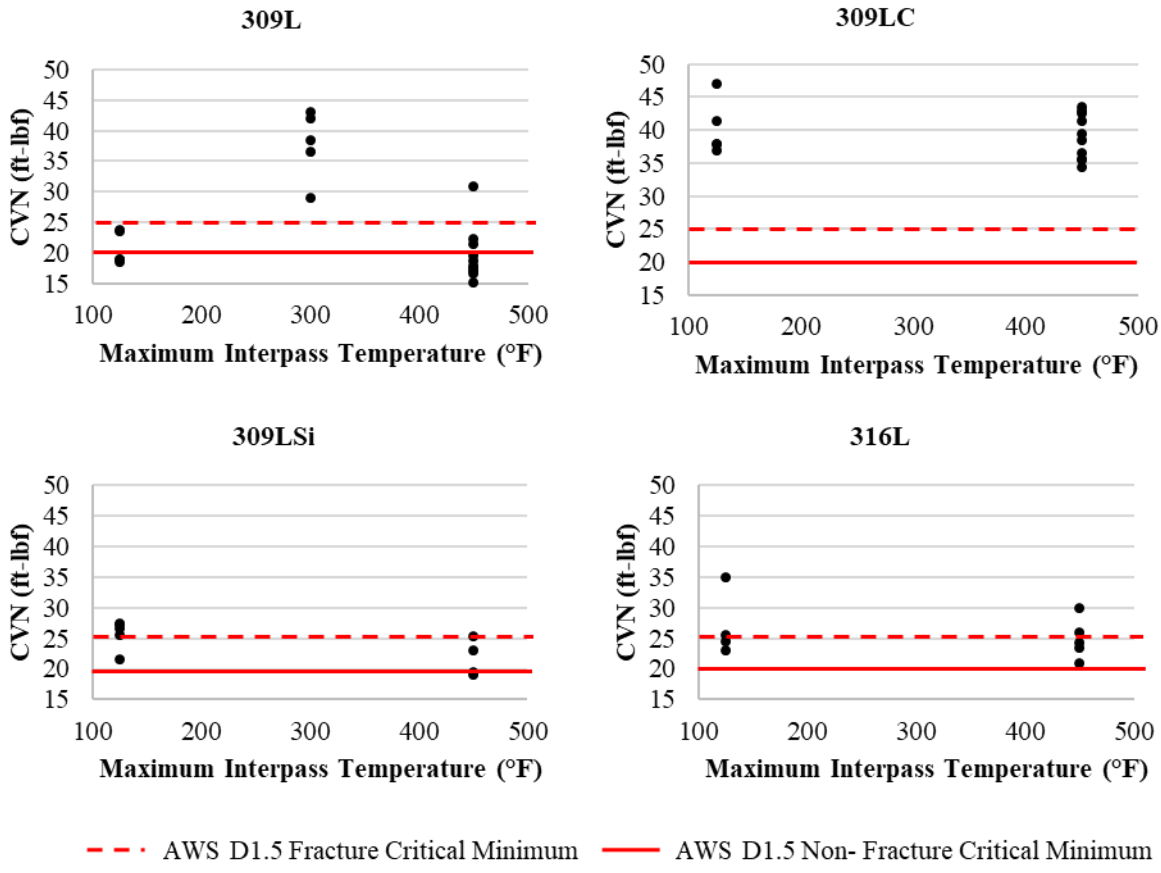

Figure D.10. CVN impact energy as a function of the maximum interpass temperature, while keeping the heat input is held constant at 75 kJ/in of all Group 1 plates

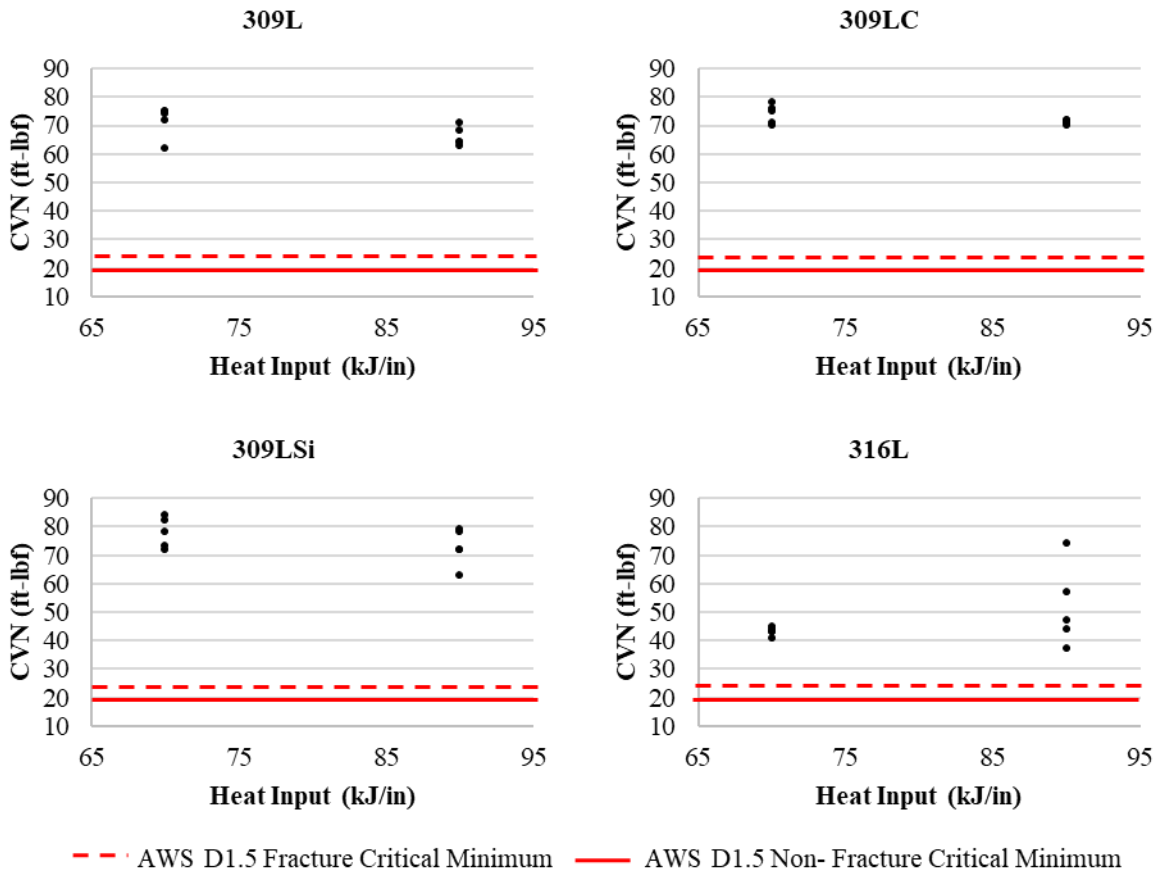

Figure D.11. CVN impact energy as a function of heat input while keeping the maximum interpass temperature constant at 300 °F on Group 2 plates

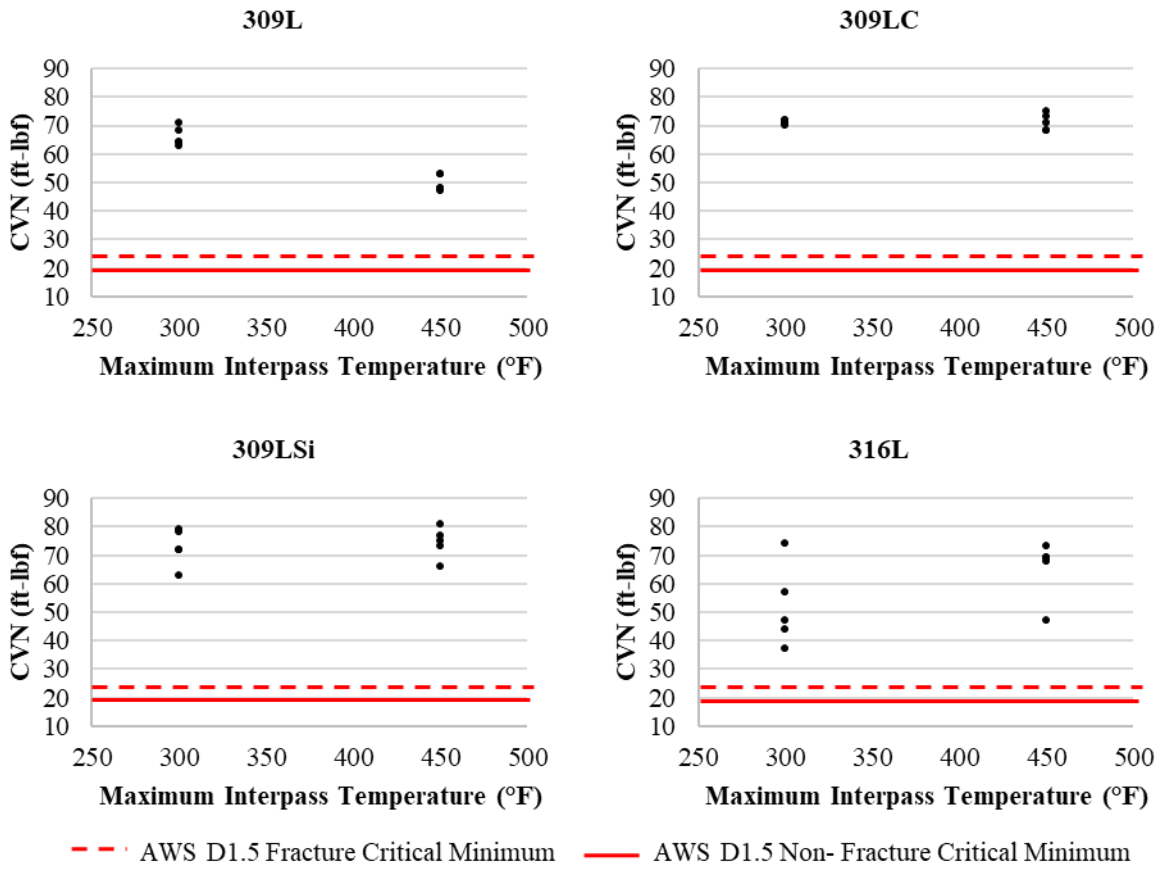

Figure D.12. CVN impact energy as a function of the maximum interpass while keeping the heat input is held constant at 90 kJ/in on Group 2 plates